Electronic Supplementary Material (ESI) for Analyst.

Supporting Information:

On the Mechanism of the Bipolar Reference Electrode

Nicole L. Walker[a], Jeffrey E. Dick[a,b,*]
[a] Department of Chemistry, Purdue University, West Lafayette, IN 47907, USA
[b] Elmore Family School of Electrical and Computer Engineering, Purdue University, West Lafayette, IN 47907, USA
[*]To whom correspondence should be addressed: jdick@purdue.edu

Table of Contents

Full Experimental Section

Chemicals and reagents. All chemicals were of analytical grade unless noted otherwise and were used as received. Ferricyanide (99.98%), ferrocyanide (≥98.5 %), ferrocene methanol (97%), 1,2-napthoquinone (97%), nitric acid (70%), Sodium phosphate monobasic monohydrate ($NaH_2PO_4{\cdot}H_2O$) (≥98 %), sodium dodecyl sulfate (SDS) (≥99%), Tetrabutylammonium hexafluorophosphate ($TBAPF_6$) (≥99.0 %), $FeCl_3$ (97%), and Luperox A98 (benzoyl peroxide (BPO)) (98%) were obtained from Sigma-Aldrich. Potassium chloride and sodium chloride (USP/FCC crystalline) were obtained from Fisher Bioreagents. Tri-n-propylamine (TPrA) (98%) was obtained from Alfa-Aesar. Tris(bipyridine)ruthenium(II) chloride ($Ru(bpy)_3Cl_2{\cdot}6H_2O$) (≥98%), lithium chloride (99%), and sodium phosphate dibasic (Na_2HPO_4) (99%) were obtained from Acros Organics. Acetonitrile (≥99.5 %) and concentrated hydrochloric acid (ACS grade) were obtained from VWR. All stock solutions were made with ultrapure water, vortexed until homogeneous using a vortex-genie (Scientific Industries, New York, Bohemia). and kept in the dark throughout use.

Instrumentation. All open electrochemical experiments, with the exception of the electrochemical impedance experiments, were performed on a CHI model 601E or 660D potentiostat (CH Instruments, Austin, TX). All electrochemical impedance spectroscopy and electrochemiluminescence experiments were performed on a Pine Research WaveDriver 200 potentiostat (Durham, NC) or a BioLogic VSP-300. Gold macroelectrodes (d = 2 mm) or ultramicroelectrodes (r = 12.5 μm), were used as working electrodes in most experiments. Silver/silver chloride reference electrodes (stored in 1M KCl) or platinum wire quasi-reference electrodes were used as the standard for comparison. A glassy carbon or graphite rod was used a counter electrode when needed. For the mechanistic studies, platinum macroelectrodes (r = 1 mm) and ultramicroelectrodes (r = 10 μm) were used to form the bridge. All electrodes were purchased from CHI (CH Instruments, Austin, TX). For all electrochemical measurements except open circuit potentiometry, a three-electrode cell was used involving a freshly polished gold macroelectrode, a glassy carbon counter electrode, and either a commercial Ag/AgCl reference electrode, a BPRE, or a platinum wire quasi-reference. Open circuit potentiometry was done using a two-electrode cell consisting of a freshly polished gold macroelectrode and either a commercial Ag/AgCl reference electrode, a BPRE, or a Pt wire quasi-reference.

Preparation of the bipolar reference electrodes (BPREs) was done as described previously[22] using a propane torch (BernzOmatic, Newark, NJ). Borosilicate glass capillary tubes were used with an outer diameter = 2.0 mm, inner diameter = 1.16 mm, length = 15 cm (Sutter Instruments, Novato, CA). Wires used were platinum (d = 0.25 mm) and silver (d = 0.25 mm) from Sigma-Aldrich, Copper tape (w = 0.25 in) was from Thermo Fisher Scientific. Graphite was Pentel Hi-Polymer pencil lead (d = 0.7 mm). Sealed quartz tips were made from quartz capillary tubes with an outer diameter of 1.0 mm, inner diameter 0.30 mm, length 15 cm, (Sutter Instruments, Novato, CA). Chipquik BPREs were fabricated using Chipquik® EGS10W-20G White Electronic Grade Silicon Adhesive Sealant (Concept to Life Solutions Inc., Ancaster, Ontario). Gorilla BPREs were fabricated using Gorilla Epoxy Clear Epoxy Adhesive (Gorilla Glue Company, Sharonville, OH).

Inductively coupled plasma-mass spectra were obtained using a NexION 300D Inductively Coupled Plasma-Mass Spectrometer (PerkinElmer, Waltham, MA) and all samples were analyzed in 2% HNO_3 using Yttrium as an internal standard. Conductivity measurements were done with a Traceable™ Conductivity Meter Pen (Fisher Scientific, Pittsburgh, PA). Scanning electron microscopy (SEM) images were collected using a Helios 600 Nanolab dual beam system (FEI, Hillsboro, OR), and energy dispersive X-ray spectroscopy (EDX) was measured using an INCA PentaFET-x3 detector (Oxford Instruments, Abingdon, UK). Flame Atomic Absorption Spectroscopy measurements were done using a AAnalyst 100 and a K-Na lamp (Perkin Elmer, Waltham, MA) at 12mA. Optical microscopy was done with an Industrial Inspection Light Microscope Micro Dyna Zoom (Bausch & Lomb, Laval, Quebec) at 40 X.

BPRE Fabrication. BPREs were fabricated as previously described[22]. Briefly, a platinum wire (d = 0.25 mm, length = 2-3 cm) was sealed in a borosilicate glass capillary tube (OD = 2.0 mm, ID = 1.16 mm) using a propane torch. The capillary tube was held in the flame until the end containing the platinum wire was molten, then it was allowed to cool to room temperature. The other end of the capillary tube was filled with 1 M KCl, then a silver wire that had been anodized[1] in 1 M HCl was placed into the back end of the tube. Copper tape was used to form an electrical connection with the exposed end of the silver wire. Parafilm was used to hold the Ag/AgCl wire in the back end of the BPRE. Graphite BPREs were made in the same way. Quartz tipped BPREs were made in the same way, but the glass tips were slowly and carefully cooled after sealing in order to prevent the glass from breaking. Chipquik BPREs or Gorilla BPREs were fabricated as described above, then were coated in Chipquik® EGS10W-20G White Electronic Grade Silicon Adhesive Sealant or Gorilla Epoxy Clear Epoxy Adhesive and left overnight to cure at 35°C. No tip BPREs were made by fully sealing the borosilicate capillary to itself with no tip material present.

Silver and Chloride Leakage Tests. Vials and BPREs were first cleaned of trace impurities by incubation in 70% HNO_3 (trace metal grade) for 24 hours, before being washed out with ultrapure water and dried. Chipquik and Gorilla BPREs were cleaned of trace impurities by soaking in a vial of ultrapure water for 15 minutes three times. Then, BPREs were filled with 1M KCl and an Ag/AgCl wire and incubated in 20 mL of ultrapure water for 30 or 31 days, as were controls BPREs containing ultrapure water only. Afterwards, the water samples were analyzed using inductively-couple plasma mass spectrometry (ICP-MS) to determine their ion concentrations.

Electrochemiluminescence. All electrochemiluminescence experiments were done using a commercial Ag/AgCl reference electrode, two pieces of platinum foil (23 mm by 28 mm, 0.05 mm thick) from Aldrich Chemical Co. as the working and counter electrodes, and a BPRE platinum wire tip placed between the two pieces of platinum foil (see **Figure S18a**). The BPRE platinum wire tip was a total of 32 mm long, with one exposed platinum end 10 mm long and the other exposed platinum end 7 mm long. Each half cell was 30 mm by 30 mm, the entire cell together was 68 mm long. The two pieces of platinum foil were about 64 mm apart.

For the $[Ru(bpy)_3]^{2+}$/TPrA reaction in water, a solution of 50 mM TPrA in 10 mM sodium phosphate buffer (pH 7.0) with 1% SDS was made with 0.5 mM $Ru(bpy)_3Cl_2 \cdot 6H_2O$. For the $[Ru(bpy)_3]^{2+}$/BPO reaction in acetonitrile, a solution of 50 mM BPO in 10 mM $TBAPF_6$ in acetonitrile was made with 0.5 mM $Ru(bpy)_3Cl_2 \cdot 6H_2O$. For the $[Ru(bpy)_3]^{2+}$/TPrA reaction in acetonitrile, 50 mM TPrA in 10 mM $TBAPF_6$ in acetonitrile was made with 0.25 mM $Ru(bpy)_3Cl_2 \cdot 6H_2O$.

Colorimetric Leakage Tests

An experiment similar to that done in a previous paper was done to visualize the leakage of smaller ions out of the BPRE. In the previous work, Anderson and co-workers used the mixing of $FeCl_3$ and SCN^- to form $Fe[(SCN)(H2O)_5]^{2+}$, a dark red complex. When a reference electrode was filled with either $FeCl_3$ or SCN^- and placed into a solution of the other, the formation of the red product was seen.[1] Similarly, here we filled three BPREs with a 2.5M $FeCl_3$ solution and placed these in solutions of 50 mM ferrocyanide for a month. As can be seen in **Figure S1**, the mixing of these two solutions immediately forms a dark blue, colloidal product called Prussian Blue[2,3]. This reaction was chosen not only because of the very dark color of the product, but because the Fe^{3+} ion is 0.049 to 0.078 nm[4], which is smaller than the Cl^-, K^+, and Ag^+ ions. When incubated in ferrocyanide over a month, there was no Prussian Blue formed at the tip of any of the BPREs, nor did any of the solutions show a blue tinge that would indicate that Prussian Blue formed in solution (**Figures S2-S4**). However, like the methylene blue experiments from the previous paper, Prussian Blue could have formed and simply be below the limit of detection using visual methods. As can be seen in **Figure S5**, addition of less than 40 µM $FeCl_3$ does not produce a visible amount of Prussian Blue, and the leakage test solutions remain yellow instead of being green- or blue-tinged as would be expected of a solution with Prussian Blue in it.

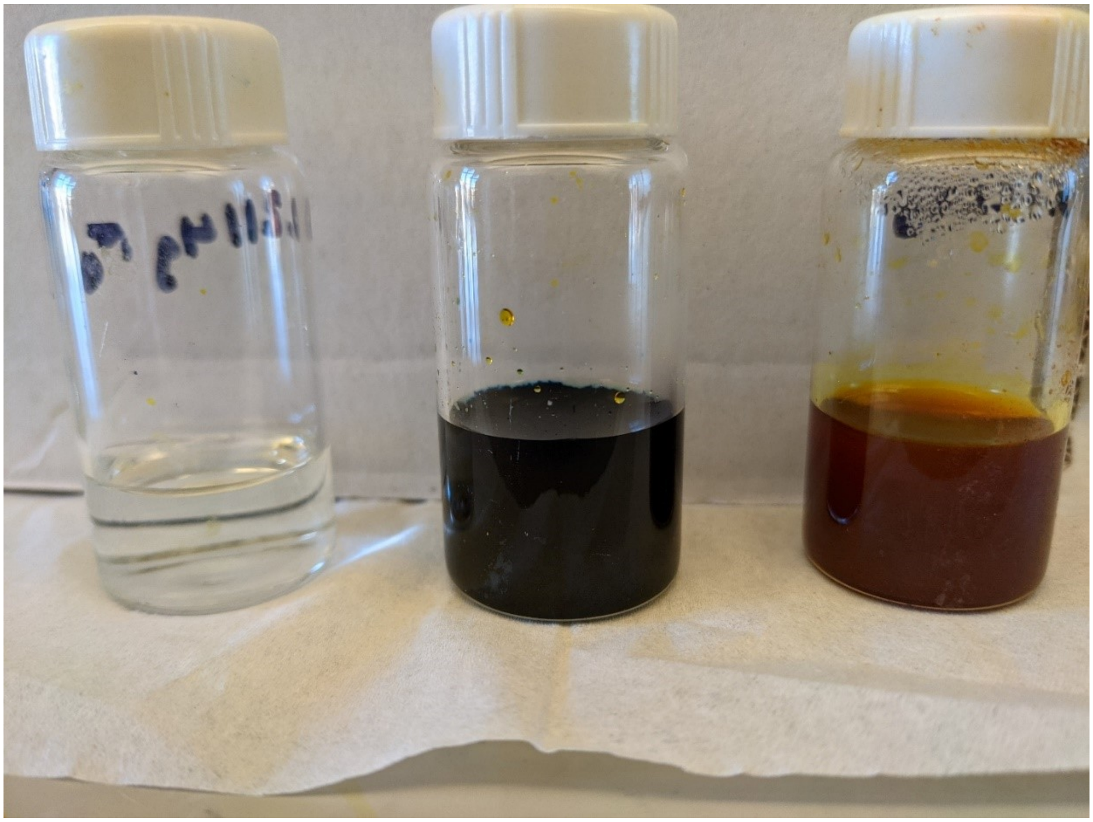

Figure S1. Prussian Blue formation. Left, a solution of 50 mM ferrocyanide in ultrapure water. Right, a solution of 2.5 M $FeCl_3$ in ultrapure water. Middle, a mixture of 5 mL of 50 mM ferrocyanide and 5 mL of 2.5 M $FeCl_3$, forming a dark blue colloidal product, Prussian Blue. Formation of the product happened immediately upon mixing the two solutions.

Prussian Blue leakage tests were done by filling three BPREs with 2.5 M $FeCl_3$ and incubating them in a 50 mM ferrocyanide solution for 30 days. If Fe^{3+} leakage into the ferrocyanide solution occurred (or ferrocyanide leakage into the BPREs), the dark blue product, Prussian Blue should be immediately formed. The color change of the solution is due to the ferrocyanide conversion to ferricyanide were not ly in the **ure S3**).

#3

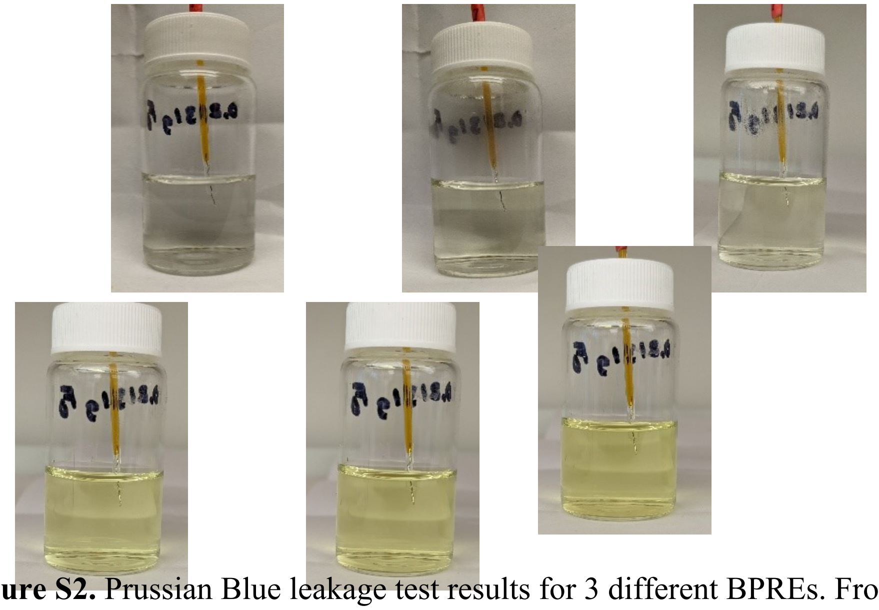

Figure S2. Prussian Blue leakage test results for 3 different BPREs. From left to right, day 0, day 1, day 2, day 9, day 15, day 30.

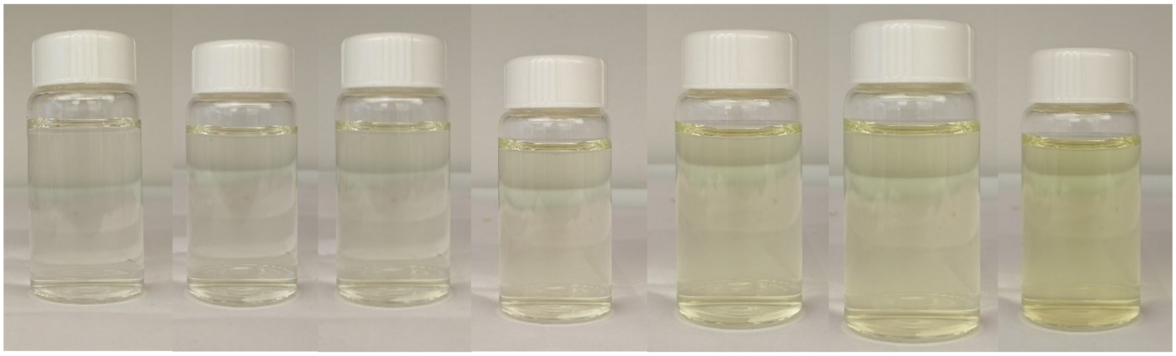

Figure S3. 50 mM ferrocyanide in ultrapure water controls. From left to right, day 0, day 1, day 2, day 5, day 9, day 15, day 29.

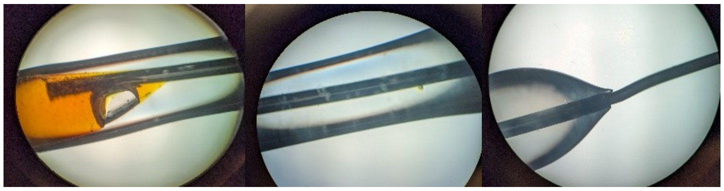

#1

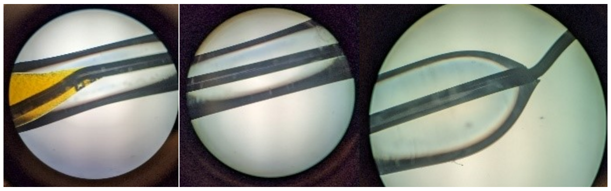

#2

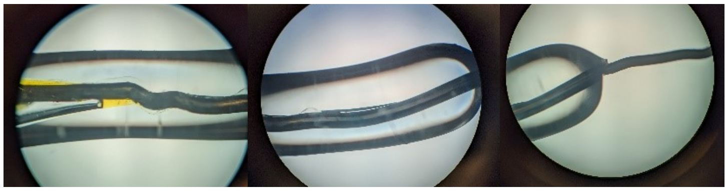

#3

Figure S4. Prussian Blue leakage test results for 3 different BPREs on day 30. From left to right, optical microscopy image (40 X) of the seal and the inner filling solution, image of the seal, and image of the seal at the tip of the BPRE after 30 days immersed in 50 mM ferrocyanide in ultrapure water. No Prussian Blue is observed at the tips.

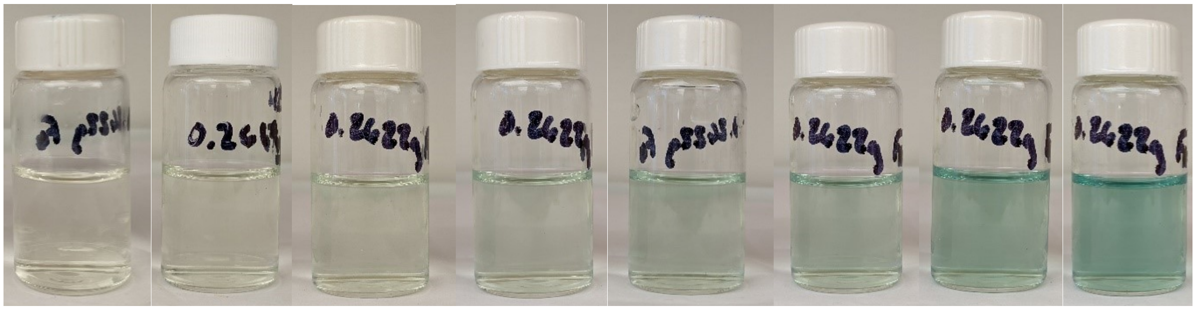

Figure S5. 50 mM ferrocyanide in ultrapure water controls with $FeCl_3$ added to make Prussian Blue. From left to right, 0 µM, 20 µM, 40 µM, 60 µM, 80 µM, 100 µM, 150 µM, 200 µM.

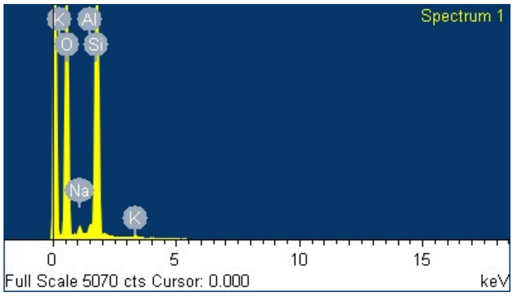

SEM-EDX Micrographs of An Unused BPRE

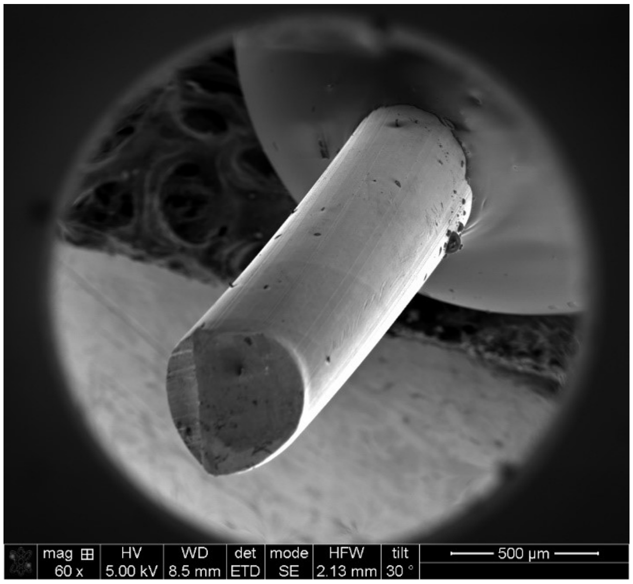

Figure S6. SEM micrographs taken of an unused BPRE

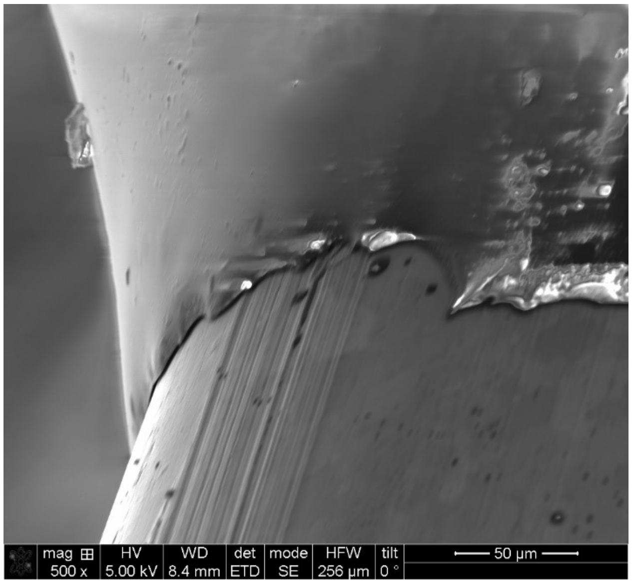

Figure S7. SEM-EDX micrographs taken of an unused BPRE, zoomed in to view the platinum-glass seal.

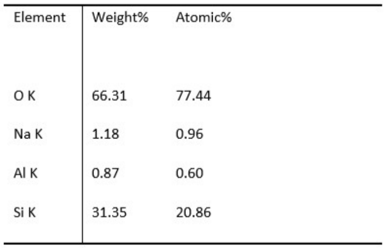

Element	Weight%	Atomic%
O K	66.31	77.44
Na K	1.18	0.96
Al K	0.87	0.60
Si K	31.35	20.86

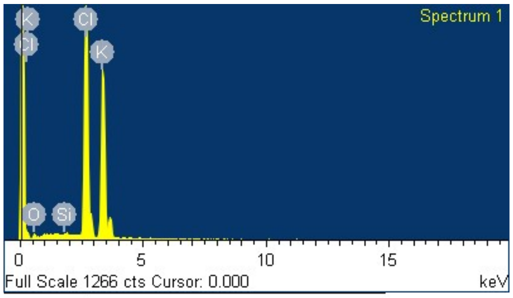

Figure S8. SEM-EDX results taken of an unused BPRE (left, top EDX spectrum) from the borosilicate glass tube and (right, bottom EDX spectrum) fo

SEM-EDX Micrographs of An BPRE with KCl Inside

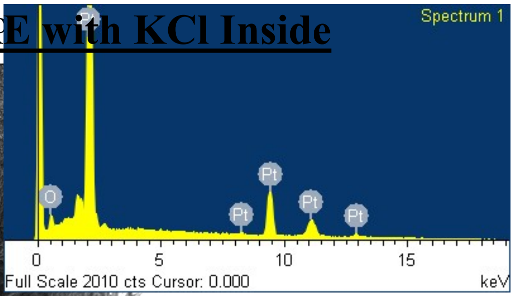

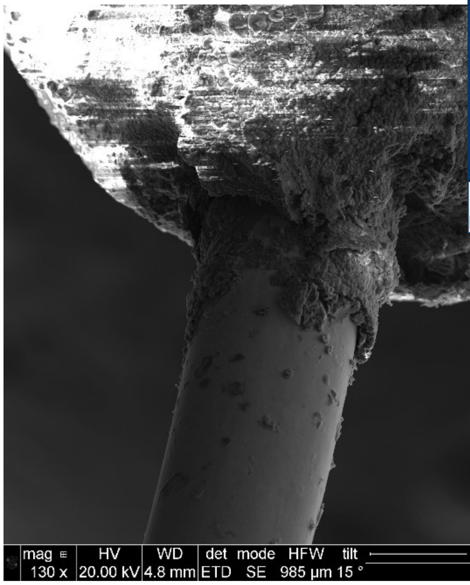

Figure S9. SEM micrographs taken of a BPRE that was filled with 1 M KCl for a week.

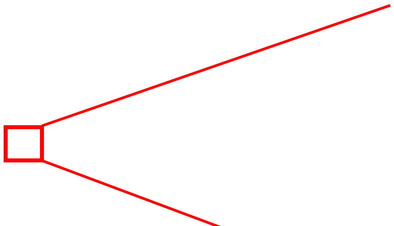

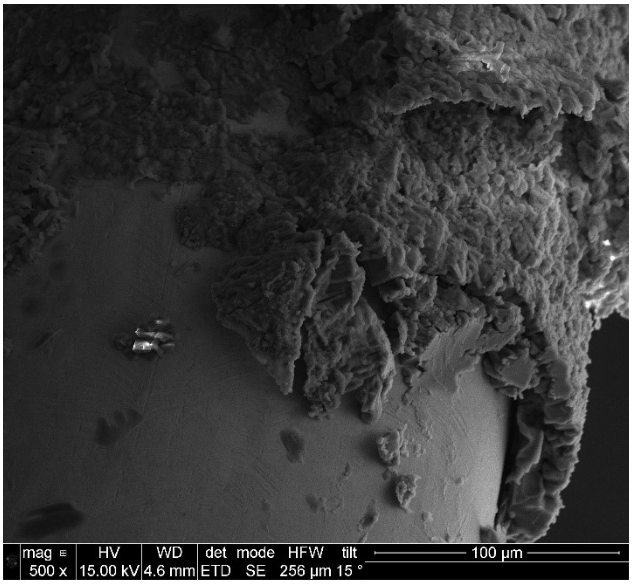

Figure S10. SEM-EDX micrographs taken of a BPRE in which KCl had incubated for one week, zoomed in to view the platinum-glass seal.

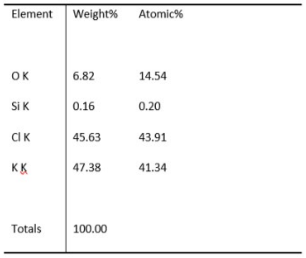

Element	Weight%	Atomic%
O K	6.82	14.54
Si K	0.16	0.20
Cl K	45.63	43.91
K K	47.38	41.34
Totals	100.00	

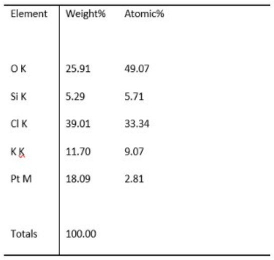

Element	Weight%	Atomic%
O K	25.91	49.07
Si K	5.29	5.71
Cl K	39.01	33.34
K K	11.70	9.07
Pt M	18.09	2.81
Totals	100.00	

Figure S11. SEM-EDX results taken of a BPRE that was f EDX spectrum) from the borosilicate glass tube and (ri platinum tip.

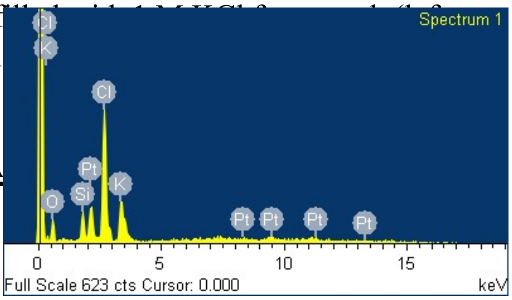

<u>Conductance, ICP-MS, and Flame A</u>

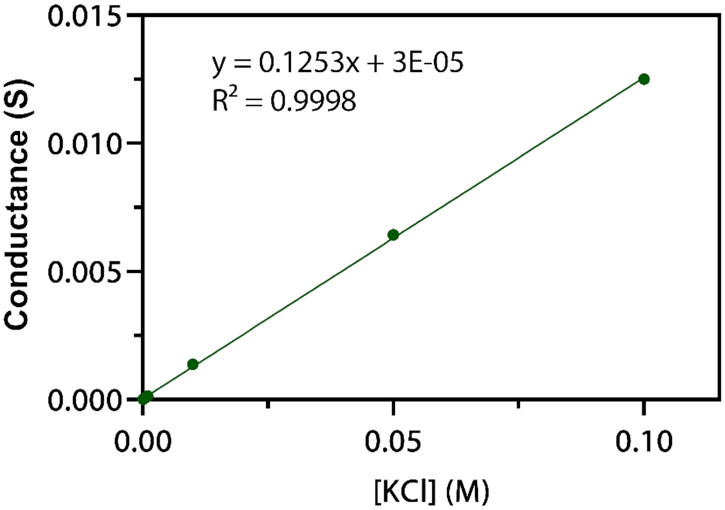

Figure S12. Calibration curve made from conductance measurements of solutions of KCl in ultrapure water (n = 5, each).

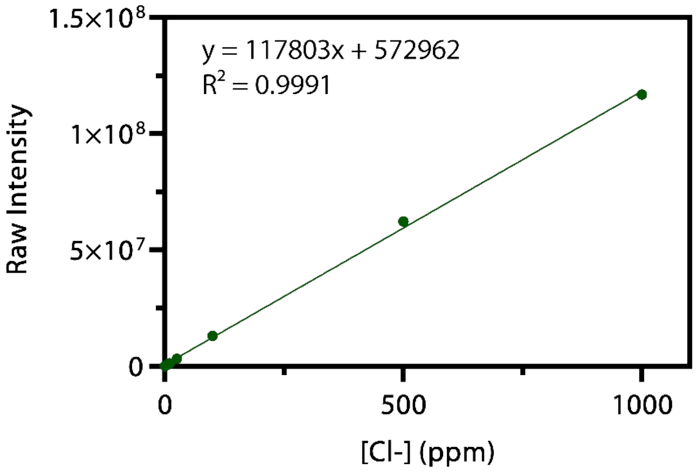

Figure S13. Cl^- Calibration curve made from ICP-MS measurements of solutions of KCl in ultrapure water, diluted with 2% HNO_3 (n = 5, each).

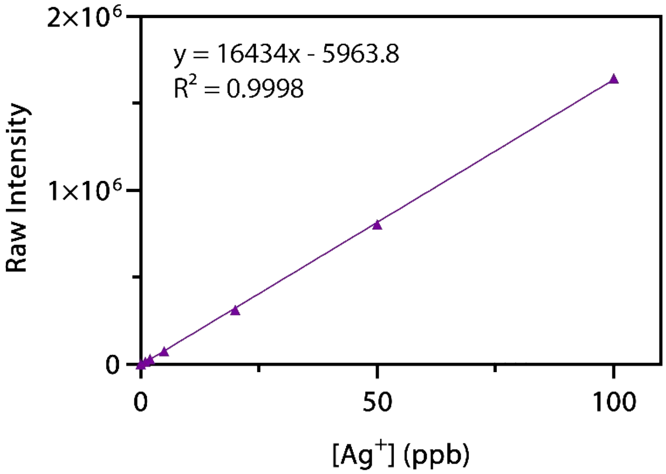

Figure S14. Ag^+ Calibration curve made from ICP-MS measurements of solutions of KCl in ultrapure water, diluted with 2% HNO_3 (n = 5, each).

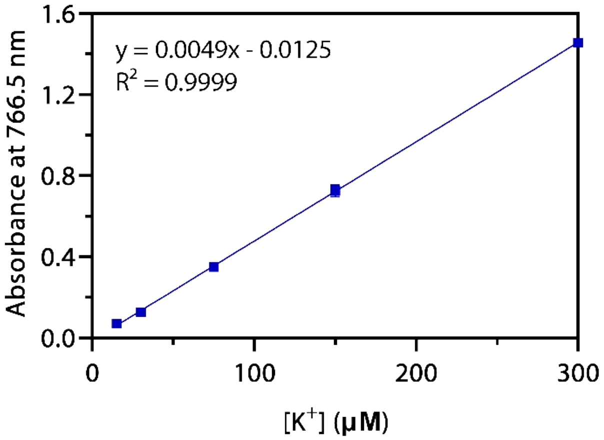

Figure S15. K^+ Calibration curve made from flame atomic absorption spectroscopy measurements of solutions of KCl in ultrapure water (n = 3, each)

Table S1. Comparison of reference electrodes mentioned in this work.

Reference Electrode	**Leakage Rate Cl^- (pmol/s)**	**Leakage Rate Ag^+ (pmol/s)**	**Resistance (kΩ)**	**Has Frit?**	**Fabrication Process**
This work	1-3.7	0.025	1.369 ± 0.706[5]	No	Fast (~5 min), Easy. Simply use a torch to melt glass around a Pt wire
Single Junction[5-7]	100	38	2.340 ± 0.403	Yes	Commercial or fast and relatively easy. Heat shrink a commercial glass frit into a glass tube.
Double Junction[7]		0.670		Yes	Fast and relatively easy. Heat shrink two commercial glass frits into two glass tubes and place one inside the other.
Vycor frit 4-6 nm pores[8]	3-4		0.069 ± 0.017	Yes	Commercial or fast and relatively easy. Heat shrink a commercial glass frit into a glass tube.
Pressure-Driven[9]	83		32,000 ± 3,000 Ω	No	Somewhat complicated and slow (24+ hours) to fabricated. Requires pump to operate.

Liquid Junction Potential Calculations

As discussed in Bard and Faulkner, a type two liquid junction is one in which two solutions are in contact that each contain an equivalent concentration of their electrolyte, but the electrolyte in each phase has only one ion in common.[10] An example of such a system is described by:

Ag/AgCl/HCl(1 M) / KCl(1 M)/AgCl/Ag Eq. 1

For a system of this type, the liquid junction potential can be described by the Lewis-Sargent relation[11]:

$$E_j = \pm \frac{RT}{F} \ln\left(\frac{\Lambda_\beta}{\Lambda_\alpha}\right) \quad \text{Eq. 2}$$

Where E_j is the junction potential (in this case, equivalent to the E_{OCP} of the system), R is the universal gas constant and T is the temperature in Kelvin, F is the Faraday, and Λ_α and Λ_β are the equivalent conductivities of the α and β phases, respectively. Here, a positive indicates that there is a common cation, and a negative indicates that there is a common anion. Since the s can be regarded as the sum of the individual equivalent ionic conductivities (λ)[10]

$\Lambda = \lambda_+ + \lambda_-$ Eq. 3

And some λ_0 values are provided[10] at 25°C, we can calcualte the theoretical junction potentials between systems similar to those in Eq. 1 as the electrolytes in both phases are changed from 1M KCl, 1M NaCl, 1M LiCl, and 1M HCl (**Table S2**). In these systems, a commercial Ag/AgCl wire is used as the working electrode in a solution of 1M electrolyte (phase α) and either a commercial Ag/AgCl reference electrode or a BPRE filled with 1M electrolyte (phase β).

Table S2. Theoretical and experimental junction potentials (n = 3).

α (1M)	β (1M)	$E_{j,theoretical}$ (mV) at 22 °C	$E_{j,experimental}$ (mV) Commercial Ag/AgCl Reference Electrode	$E_{j,experimental}$ (mV) BPRE
HCl	KCl	-26.5	-26.2 ± 2.3	-24.6 ± 2.4
KCl	KCl	0	1.5 ± 0.9	1.8 ± 1.5
NaCl	KCl	4.3	7.7 ± 1.4	8.5 ± 1.8
LiCl	KCl	6.7	10.0 ± 1.5	11.7 ± 2.4
KCl	HCl	26.5	25.3 ± 3.3	24.6 ± 3.4
KCl	KCl	0	1.5 ± 0.9	1.8 ± 1.5
KCl	NaCl	-4.3	-6.8 ± 0.7	-6.8 ± 0.8
KCl	LiCl	-6.7	-9.9 ± 1.0	-10.0 ± 2.3

Statistically, a series of student's t-tests shows that the experimental E_j values for commercial Ag/AgCl references and BPREs are statistically insignificantly different under all conditions tested.

Epoxy and Glue Tests

One end of an unsealed capillary (Outer diameter = 2 mm, inner diameter = 1.16 mm) was covered thickly with a layer of one of the epoxies or glues listed below in Table S1. These capillaries were cured at either 85°C (inside of a temperature-controlled oven) or at 35°C (by placing the capillaries on top of the temperature-controlled oven) overnight.

Table S3. Epoxies and Glues Tested and Their Curing Temperatures

Epoxy or Glue Name	**Curing Temperature (°C)**
Gorilla Epoxy Clear Epoxy Adhesive	35
Loctite Glass Glue	85
Epon Resin 815C + 12% (v/v) Epikure Curing Agent 3223 (Miller-Stephenson)	85
Epon Resin 828 + 12% (v/v) Epikure Curing Agent 3223 (Miller-Stephenson)	85
Epoxylite® E 6001 (Elantas)	85
Gorilla 100% Silicone Clear Sealant	35
White Gorilla Glue	35
Permatex Ultra Black Maximum Oil Resistance RTV Silicone Gasket Maker	35
Chipquik® EGS10W-20G White Electronic Grade Silicon Adhesive Sealant	35
Loctite Epoxy Translucent Yellow	35
J. B. Kwikweld: J. B. Kwik Epoxy Resin + Epoxy Hardener	35

Three of each type of sealed capillary tube were filled with 3M KCl in ultrapure water, then all three were placed into one vial of 20mL of ultrapure water for 30 days. Three of each type of sealed capillary tube were filled with 15.2 mM methylene blue in ultrapure water, then all three were placed into one vial of 20mL of ultrapure water for 30 days. Five vials of ultrapure water were also left for 30 days as a control.

Periodically, throughout the 30 day incubation, the conductivity of the water samples with the KCl-filled capillaries were measured to determine if any KCl had leaked out through the epoxy/glue (**Figure S16**). Throughout this 30 day incubation, the water in which the methylene blue-filled capillaries were incubated was visually inspected to determine if any methylene blue was able to leak through the epoxy/glue layer. These tests established that methylene blue did not visibly leak through any of the epoxies/glues in this time period (**Figure S17**).

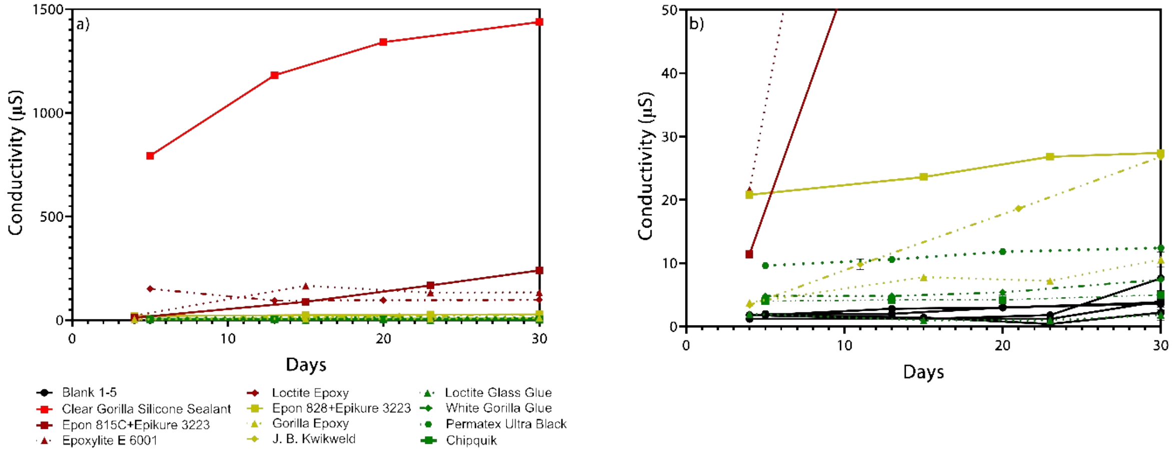

Figure S16. a) Conductivity measurements of vials of water in which 3M KCl-filled capillaries sealed with various epoxies or glues were incubated for 30 days. **b)** a zoomed in view showing the lowest leakage samples.

Figure S17. Pictures taken of vials of water in which 15.2 mM methylene blue-filled capillaries sealed with various epoxies or glues were incubated after 30 days. Row 1, from left to right: Gorilla Epoxy Clear Epoxy Adhesive, Loctite Glass Glue, Epon Resin 815C + 12% (v/v) Epikure Curing Agent 3223 (Miller-Stephenson), Epon Resin 828 + 12% (v/v) Epikure Curing Agent 3223 (Miller-Stephenson), Epoxylite® E 6001 (Elantas). Second Row, from left to right: Gorilla 100% Silicone Clear Sealant, White Gorilla Glue, Permatex Ultra Black Maximum Oil Resistance RTV Silicone Gasket Maker, Chipquik® EGS10W-20G White Electronic Grade

Silicon Adhesive Sealant, Loctite Epoxy Translucent Yellow, J. B. Kwikweld: J. B. Kwik Epoxy Resin + Epoxy Hardener.

Bipolar Electrochemiluminescence Experiments

To demonstrate that the wire tip of a BPRE could be used as a bipolar electrode under conditions in which no ion transfer is possible, traditional bipolar electrochemical reactions were carried out using a BPRE's sealed platinum wire tip as the bipolar electrode (BPE) in a closed bipolar cell (see **Figure S18a**). This was realized through the use of two separate, rectangular prism cells with a small hole on one side. Through this hole, the sealed BPRE wire tip was inserted such that the ends of the platinum stuck out into the center of the cell. On the opposite end of each cell a large piece of platinum foil was placed, and one cell contained a commercial Ag/AgCl reference electrode. Then, electrochemiluminescence reactions were driven at the ends of the BPRE by applying a potential across the feeder electrodes, creating an electric field along the length of the platinum wire tip of the BPRE.

In the first reaction, electrochemiluminescence was driven at one end of the BPRE wire tip using the anodic co-reactant method of tri-n-propylamine (TPrA) and $[Ru(bpy)_3]^{2+*}$. The exact mechanism of this reaction depends on a number of reaction conditions[12,13], but overall, the heterogeneous oxidation of either TPrA and/or $[Ru(bpy)_3]^{2+}$ results in homogeneous electron transfer to produce the excited species $[Ru(bpy)_3]^{2+*}$. In pH 7.0 sodium phosphate buffer, the application of +2.5 V to the feeder electrodes causes ECL to occur, while the cathodic reaction is the reduction of H^+ to H_2 gas[14,15] (**Figure S18b**). By switching the applied potential between -2.5 V and 2.5 V, ECL can be seen to switch sides of the BPRE wire tip (**Video S1**). The H_2 bubbles are harder to see, however, so a different reaction was chosen that would be visualized more easily.

For the second reaction, electrochemiluminescence was driven at both ends of the electrode. At one end, the same $[Ru(bpy)_3]^{2+}$/TPrA anodic co-reactant method was used, resulting in a bright ECL signal when 7.65 V was applied. In the other cell, a $[Ru(bpy)_3]^{2+}$/BPO cathodic co-reaction method[16] was used, which resulted in a smaller ECL signal due to the shorter length of the exposed platinum wire on this side. In this reaction, which like the $[Ru(bpy)_3]^{2+}$/TPrA reaction has multiple possible mechanisms[17,18], reduction of BPO results the formation of a strong oxidant that can react with the reduced form of $[Ru(bpy)_3]^{2+}$ to produce ECL. When a potential of 7.65 V is applied, ECL is observed at both ends of the BPRE wire tip (**Figure 18c**). When this potential is switched between 7.65 V and 0 V, the ECL can be seen to switch on and off (**Video S2**).

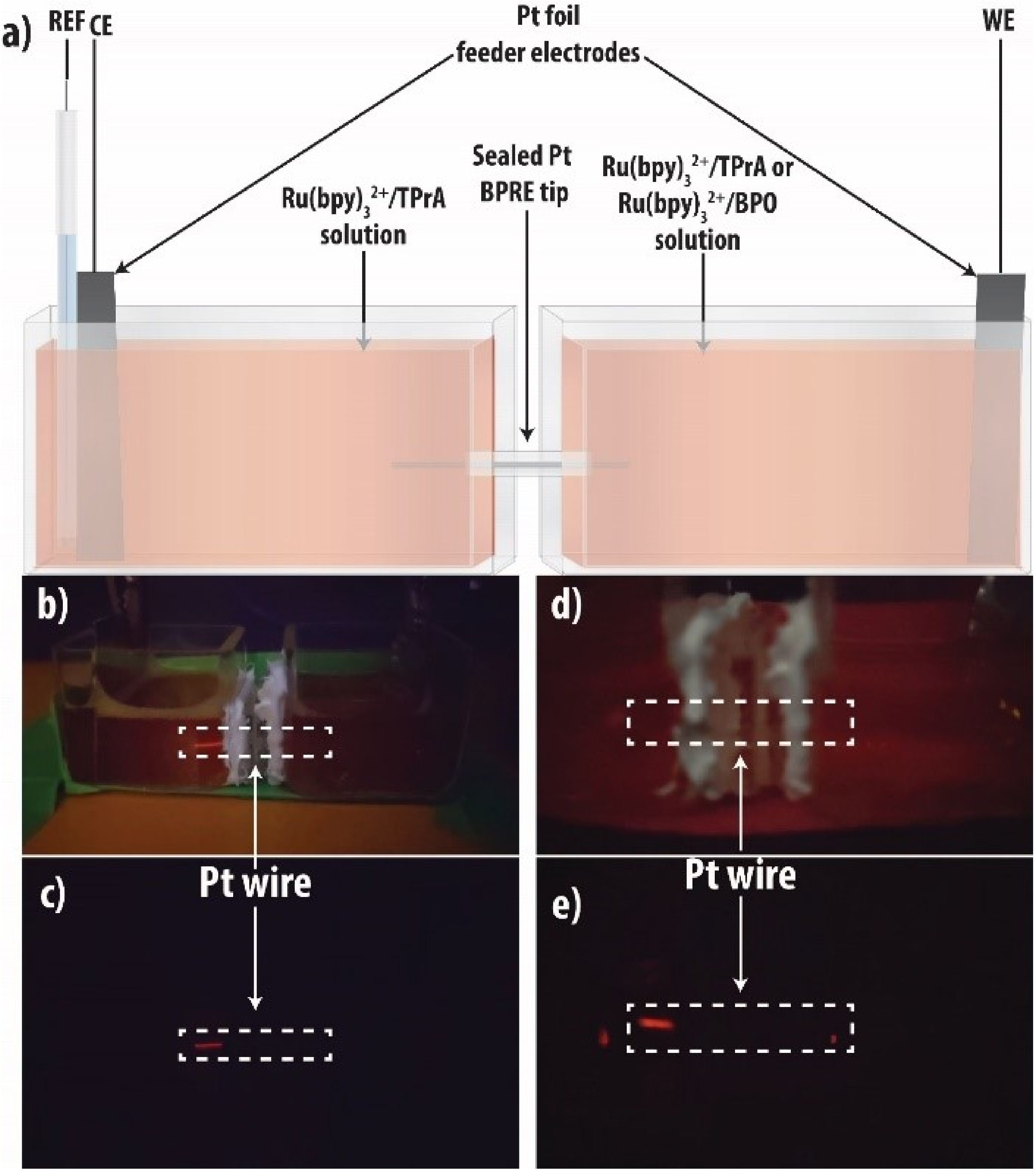

Figure S18. a) Bipolar electrochemical experiment set-up, with the BPRE wire tip placed between the two cells. **b)** Still from Video S1, showing the ECL signal on one pole the BPRE when 2.5V was applied in the light and **c)** in the dark. **d)** Still from Video S2, showing the cell before potential was applied in the light, and **e)** showing the ECL signal on both poles of the BPRE in the dark after 7.65V was applied.

For the $[Ru(bpy)_3]^{2+}$/TPrA reaction, a solution of 50 mM TPrA in 10 mM sodium phosphate buffer (pH 7.0) with 1% SDS was made with 0.5 mM $Ru(bpy)_3Cl_2{\cdot}6H_2O$ was put into both cells of the bipolar electrochemical set-up shown in Figure S18a. Two pieces of platinum foil (23 mm by 28 mm, 0.05 mm thick) as the working and counter electrodes, and a BPRE tip placed between the two cells. The BPRE tip was a total of 32 mm long, with one exposed platinum end 10 mm long and the other exposed platinum end 7 mm long. Each half cell was 30 mm by 30 mm, the entire cell together was 68 mm long. The two pieces of platinum foil were about 64 mm apart.

Application of a potential of 2.5 V for 3 seconds, followed by 0 V for 3 seconds, followed by -2.5 V for 3 seconds, followed by 0 V for 3 seconds repeats numerous times throughout the video. As the potential switches from positive to negative, the pole of the BPRE that performs the anodic ECL reaction and the one that performs the cathodic H_2 generation switches. The ECL can be seen to switch poles of the BPRE tip every 6 seconds.

Video S1. An example of the first set of ECL experiments, where both poles of the BPRE are alternately doing anodic $[Ru(bpy)_3]^{2+}$/TPrA ECL and cathodic H_2 generation.

For the $[Ru(bpy)_3]^{2+}$/TPrA reaction, a solution of 50 mM TPrA in 10 mM $TBAPF_6$ in acetonitrile was made with 0.25 mM $Ru(bpy)_3Cl_2{\cdot}6H_2O$ and put into the lefthand cell of the bipolar electrochemical set-up shown in Figure 3a. For the $[Ru(bpy)_3]^{2+}$/BPO reaction, a solution of 50 mM BPO in 10 mM $TBAPF_6$ in acetonitrile was made with 0.25 mM $Ru(bpy)_3Cl_2{\cdot}6H_2O$ and put into the righthand cell of the electrochemical set-up shown in Figure S18a. Two pieces of platinum foil (23 mm by 28 mm, 0.05 mm thick) as the working and counter electrodes, and a BPRE tip placed between the two cells. The BPRE tip was a total of 32 mm long, with one exposed platinum end 10 mm long and the other exposed platinum end 7 mm long. Each half cell was 30 mm by 30 mm, the entire cell together was 68 mm long. The two pieces of platinum foil were about 64 mm apart.

Application of a potential of 7.65 V for 3 seconds, followed by 0 V for 3 seconds, followed by 7.65 V for 3 seconds, followed by 0 V for 3 seconds repeats numerous times throughout the video. When the potential is applied, a strong ECL signal can be seen on the lefthand pole of the BPRE due to the $[Ru(bpy)_3]^{2+}$/TPrA reaction, while a shorter ECL signal can be seen on the righthand pole of the BPRE due to the shorter exposed end of the platinum wire on that side of the cell. These ECL signals switch on and off as the potential is alternately applied and reduced to 0 V.

Video S2. An example of the second set of ECL experiments, where the lefthand pole of the BPRE is doing anodic $[Ru(bpy)_3]^{2+}$/TPrA ECL and the righthand pole is doing cathodic $[Ru(bpy)_3]^{2+}$/BPO ECL.

$E_{1/2}$ Values for Various Systems Tested

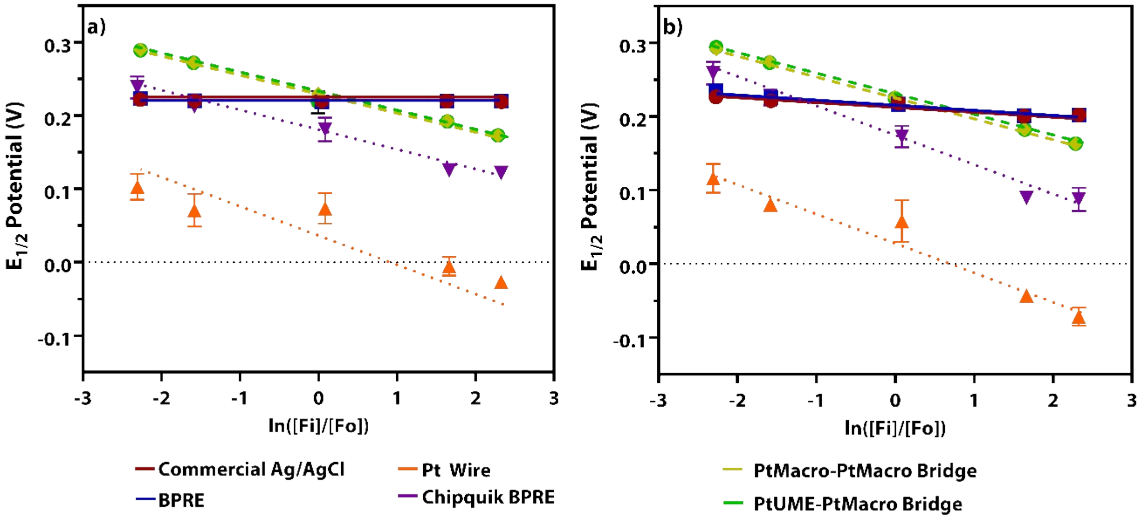

Figure S19. Relationship between ln([Ferricyanide]/[Ferrocyanide]) and the $E_{1/2}$ value of solutions of 1:10 – 10:1 ferri:ferrocyanide in 250mM KCl when using various types of reference electrodes (commercial Ag/AgCl (**red**), BPRE (**blue**), Pt wire quasi-reference (**orange, dotted**), and Chipquik BPRE (**purple, dotted**)) or the set-up described in Figure 5 of the manuscript when the working electrode is either a gold **a)** macroelectrode (**yellow, dashed**) or **b)** ultramicroelectrode (**green, dashed**).

Table S4. Line of best fit information for the data presented in Figure S19a.

Set-up used	**Line of best fit**	**R^2**
Commercial Ag/AgCl Reference Electrode	y = -0.0004x + 0.2204	0.7449
BPRE	y = -0.0006x + 0.2207	0.4619
Pt wire quasi-reference	y = -0.0265x + 0.0441	0.8921
Chipquik BPRE	y = -0.0257x + 0.1768	0.9834
2 vials, PtMacro-PtMacro Bridge (see **Figure 4a**)	y = -0.0253x + 0.2323	0.9986
2 vials, PtUME-PtMacro Bridge (see **Figure 4a**)	y = -0.0253x + 0.2295	0.9847

Table S5. Line of best fit information for the data presented in Figure S19b.

Set-up used	**Line of best fit**	**R^2**
Commercial Ag/AgCl Reference Electrode	y = -0.0074x + 0.2165	0. 9715
BPRE	y = -0.0057x + 0.214	0.9190
Pt wire quasi-reference	y = -0.0397x + 0.0295	0.9509
Chipquik BPRE	y = -0.0387x + 0.1684	0.9850
2 vials, PtMacro-PtMacro Bridge (see **Figure 4a**)	y = -0.0283x + 0.2278	0.9994
2 vials, PtUME-PtMacro Bridge (see **Figure 4a**)	y = -0.0285x + 0.2279	0.9989

OCP and CV Responses for Chipquik BPREs and Pt Wire Quasi-Reference Electrodes

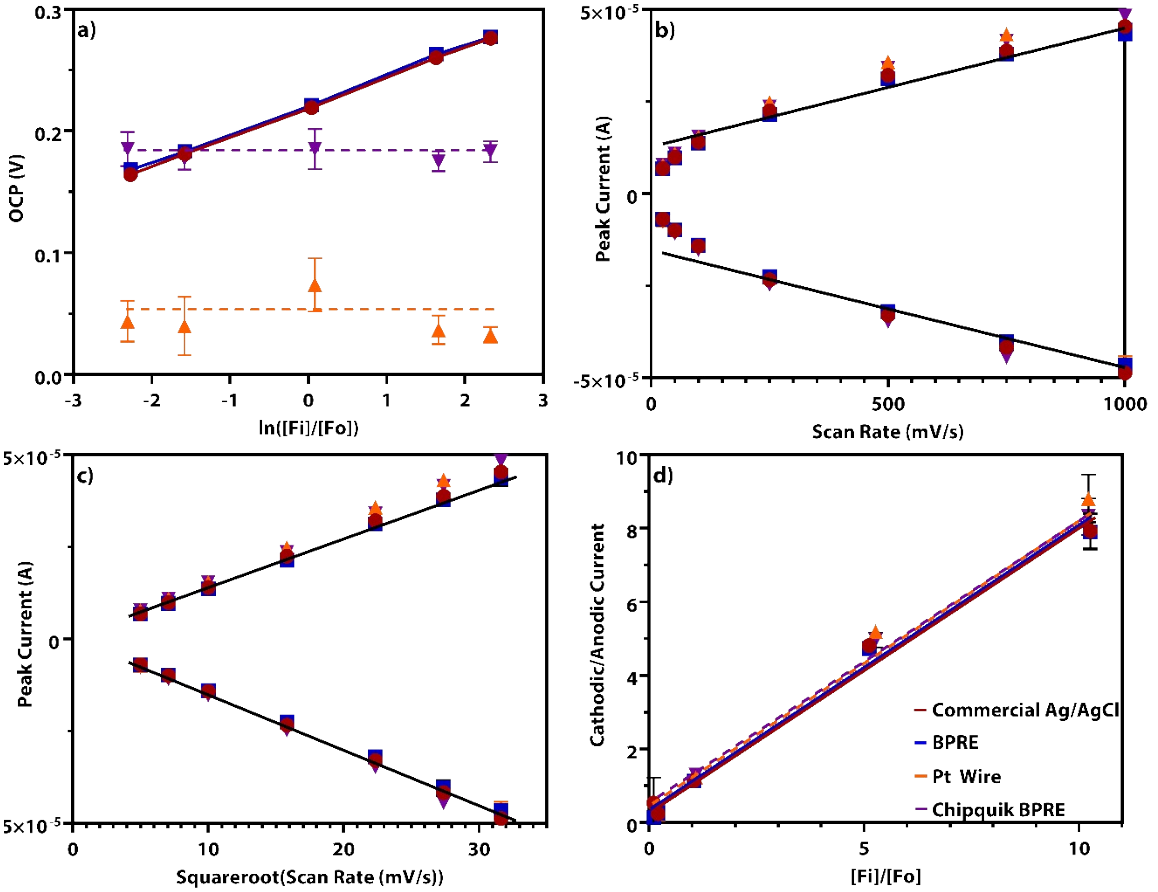

Figure S20. a) open circuit potentiometric or **b-d)** cyclic voltammetric responses using either a commercial Ag/AgCl reference electrode (**red**), a BPRE (**blue**), a Pt wire quasi-reference electrode (**orange, dashed**), or a Chipquik BPRE (**purple, dashed**) in a conventional 3-electrode cell with a gold macroelectrode as the working electrode. Relationship between **a)** open circuit potential and ln([ferricyanide]/[ferrocyanide]), **b)** scan rate or **c)** square root of scan rate and peak current on a gold macroelectrode, and **d)** [ferricyanide]/[ferrocyanide] and cathodic/anodic current on a gold ultramicroelectrode.

OCP and CV with a Pt Wire Quasi-Reference Electrode

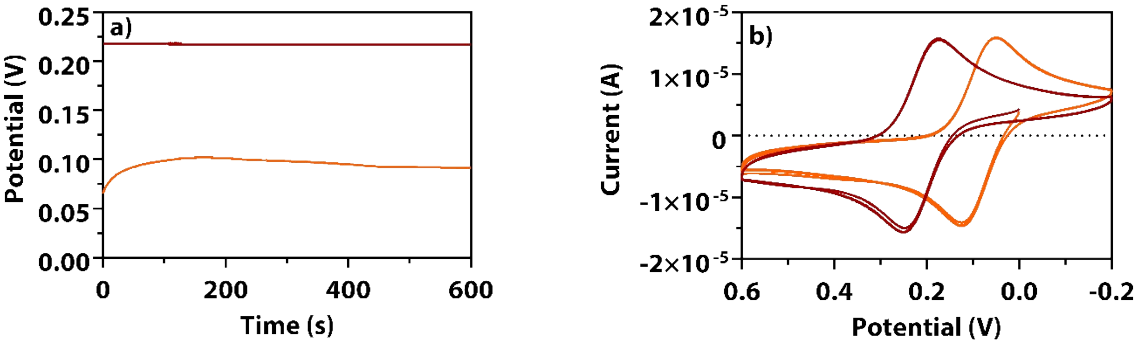

Figure S21. a) open circuit potentiometric or **b)** cyclic voltammetric responses using either a commercial Ag/AgCl reference electrode (**red**) or a Pt Wire quasi-reference electrode (**orange**) in a solution of 1:1 ferri:ferrocyanide in 250 mM KCl with a gold macroelectrode as the working electrode.

OCP Results of Commercial References, BPREs, Chipquik BPREs, and Pt Wire Quasi-Reference Electrodes

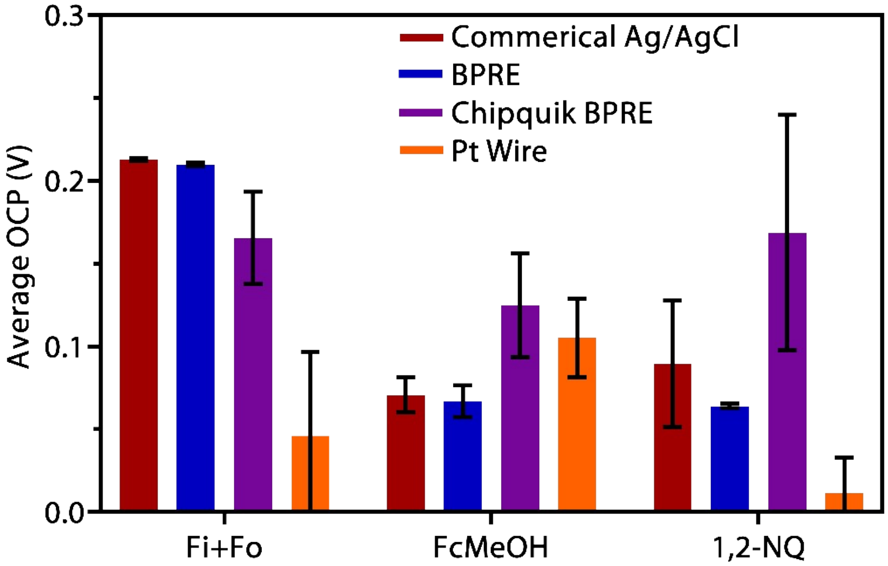

Figure S22. The average open circuit potentiometric response over 5 minutes using either a commercial Ag/AgCl reference electrode (**red**, n = 3), a BPRE (**blue**, n = 6), a Chipquik BPQRE (**purple**, n = 3), or a Pt Wire quasi-reference electrode (**orange**, n = 3) in a solution of either 1:1 ferri:ferrocyanide in 250 mM KCl, 2 mM ferrocene methanol in 250mM KCl, or 2mM 1,2-naphthoquinone in 250mM KCl with a gold macroelectrode as the working electrode.

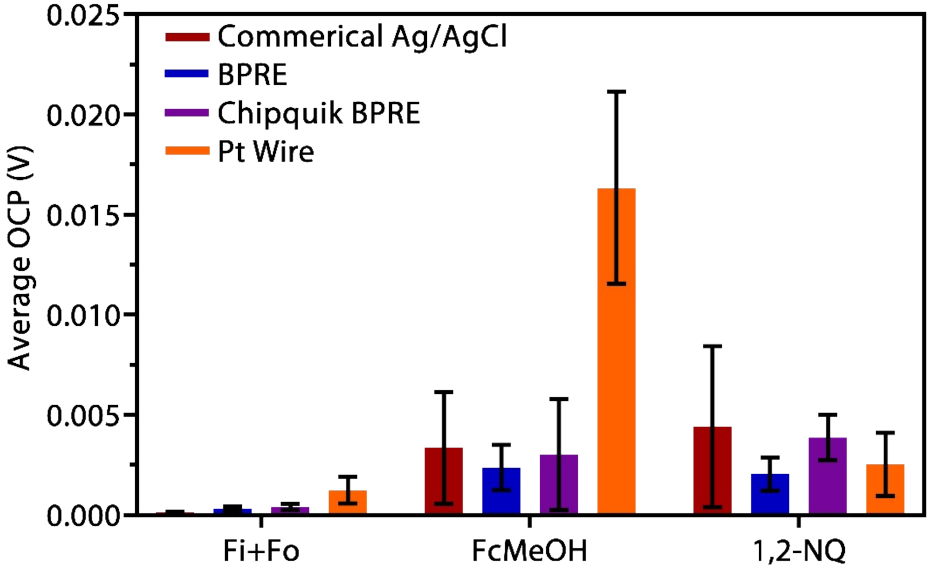

Figure S23. The standard deviation of the open circuit potentiometric response over 5 minutes using either a commercial Ag/AgCl reference electrode (**red**, n = 3), a BPRE (**blue**, n = 6), a Chipquik BPQRE (**purple**, n = 3), or a Pt Wire quasi-reference electrode (**orange**, n = 3) in a solution of either 1:1 ferri:ferrocyanide in 250 mM KCl, 2 mM ferrocene methanol in 250mM KCl, or 2mM 1,2-naphthoquinone in 250mM KCl with a gold macroelectrode as the working electrode. This standard deviation is indicative of the amount of potential drift over the 5 minute open circuit potential run.

CV Results of Commercial References, BPREs, Chipquik BPREs, and Pt Wire Quasi-Reference Electrodes

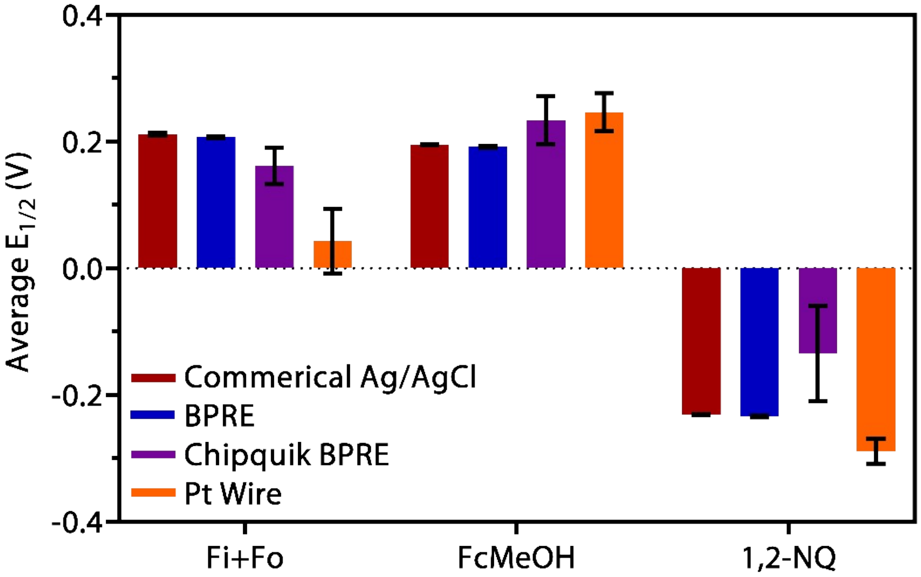

Figure S24. The average half-wave potential ($E_{1/2}$) of a cyclic voltammogram taken using either a commercial Ag/AgCl reference electrode (**red**, n = 3), a BPRE (**blue**, n = 6), a Chipquik BPQRE (**purple**, n = 3), or a Pt Wire quasi-reference electrode (**orange**, n = 3) in a solution of either 1:1 ferri:ferrocyanide in 250 mM KCl, 2 mM ferrocene methanol in 250mM KCl, or 2mM 1,2-naphthoquinone in 250mM KCl with a gold macroelectrode as the working electrode.

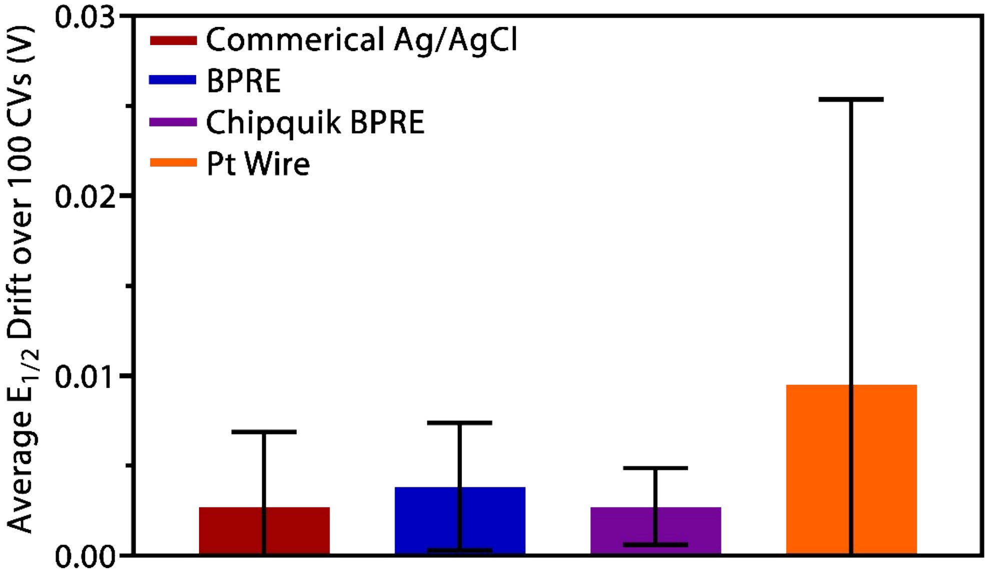

Figure S25. The average drift in half-wave potential ($E_{1/2}$) of 100 consecutive cyclic voltammograms taken using either a commercial Ag/AgCl reference electrode (**red**, n = 3), a BPRE (**blue**, n = 6), a Chipquik BPQRE (**purple**, n = 3), or a Pt Wire quasi-reference electrode (**orange**, n = 14) in a solution of either 1:1 ferri:ferrocyanide in 250 mM KCl with a gold macroelectrode as the working electrode.

Complete Mathematical Derivation of Open Circuit Potential in a Mixed System

When one describes the equilibrium potential, the equilibrium is reached when the rate of oxidation is the same as the rate of reduction. Thus, the net rate of electrons into the electrode equals the net rate of electrons going out of the electrode, and this rate, termed the exchange current (i_0), is described by the rate constant, k^0. In reality, one must also take into consideration the directionality of the bias current, which becomes important when reactions setting the open circuit potential are sufficiently slow enough such that a femtoampere (10^{-15} A) bias current becomes appreciable. We can define expressions for the current going into and out of an electrode. Consider the magnitude of the anodic and cathodic (i_A and i_C, respectively) exchange currents:

$$|i_A| = n_A F A k_A^o C_{R\,(x=0)} e^{(1-\alpha_A) f (E_{OCP} - E_A^0)} \qquad \text{Eq. 4}$$

$$|i_C| = n_C F A k_C^o C_{O\,(x=0)} e^{-\alpha_C f (E_{OCP} - E_C^0)} \qquad \text{Eq. 5}$$

where n is the number of electrons contributing to the anodic or cathodic reaction, F is the Faraday, A is the area of the electrode, $C_{R(x=0)}$ and $C_{O(x=0)}$ are the concentrations of R and O at the electrode surface, respectively, α is the transfer coefficient, and $f = \frac{F}{RT} = {\sim}39$, where R is the universal gas constant and T is the temperature in Kelvin. These reactions constitute the generalized exchange currents occurring from two separate half reactions, and the equilibrium condition is $|i_C| = |i_A|$. Again, depending on the directionality of the bias current, one would add or subtract the bias current from each of these currents and treat it as a constant current electrolysis. We have chosen to ignore contributions of the bias current within this model. We can represent the surface concentrations of O and R in more measurable quantities by considering the fractions of the currents contributing to the *OCP* measurement to the mass transfer limited currents:

$$C_{O(x=0)} = C_O^* \left(\frac{i_{dC} - i_C}{i_{dC}} \right) \qquad \text{Eq. 6}$$

$$C_{R(x=0)} = C_R^* \left(\frac{i_{dA} - i_A}{i_{dA}} \right) \qquad \text{Eq. 7}$$

where C_O* and C_R* are the bulk concentrations of O and R, respectively, and i_{dC} and i_{dA} are the mass transfer limited currents, given by:

$$i_{dC} = n_C F A m_O C_O^* \qquad \text{Eq. 8}$$

$$i_{dA} = n_A F A m_R C_R^* \qquad \text{Eq. 9}$$

where m_O and m_R are the mass transfer coefficients for species O and R in cm•s^{-1}. Mass transfer limited currents occur because the electron transfer becomes limited by the rate at which analyte species are brought to the electrode (i.e., electrons can be transferred only as quickly as analyte species are brought to the electrode). Combining these equations, we find:

$$|i_A| = n_A F A k_A^o C_O^* \left(\frac{i_{dC} - i_C}{i_{dC}}\right) e^{(1 - \alpha_A) f (E_{OCP} - E_A^0)}$$ Eq. 10

$$|i_C| = n_C F A k_C^o C_R^* \left(\frac{i_{dA} - i_A}{i_{dA}}\right) e^{- \alpha_C f (E_{OCP} - E_C^0)}$$ Eq. 11

Solving for i_A and i_C, we arrive at the following general expressions for the anodic and cathodic currents:

$$|i_C| = i_{dC}\left[1 + \frac{m_O}{k_C^0} e^{\alpha_C f \left(E_{OCP} - E_C^0\right)}\right]^{-1}$$ Eq. 12

$$|i_A| = i_{dA}\left[1 + \frac{m_R}{k_A^0} e^{-(1 - \alpha_A) f \left(E_{OCP} - E_A^0\right)}\right]^{-1}$$ Eq. 13

From Equations 9 and 10, it is algebraically cumbersome to solve for E_{OC}. While these equations can be solved for E_{OC} iteratively, the iteration itself can be cumbersome without programming techniques. The denominator of Eq. 12 & 13 can be dominated by the ratio of the mass transfer coefficient to the electron transfer kinetic rate constant if m is maximized and k^0 is minimized. The mass transfer coefficients depend on molecular diffusivity and the electrode size and can be calculated for a disk geometry using $m = \frac{4D}{\pi a}$, where D is the diffusion coefficient of O or R and a is the radius of the electrode. Use of small electrodes (experimentally feasible electrodes constitute radii greater than 10 nm) maximizes this term. One may also experimentally choose an electrochemically inert electrode material to minimize the k^0 for several reactions; however, nanoelectrodes of different materials are difficult to fabricate. For instance, the reduction of hydronium to hydrogen gas occurs at much more negative potentials on carbon compared to platinum (> 0.5V). From these considerations, we have developed a rational approach for neglecting 1 by assuming the term under in the denominator being added to 1 is at least 100x larger. By neglecting 1 and setting Equations 12 and 13 equal and solving for E_{OC}, we arrive at the general expression for the E_{OC} in a mixed, two-component system[19]:

$$E_{OCP} = \frac{\ln\left[\frac{n_C k_C^0 C_O^*}{n_A k_A^0 C_R^*}\right] + f[(1 - \alpha)E_A^0 + \alpha_C E_C^0]}{f(1 - a_A + \alpha_C)}$$ Eq. 14

This equation, while derived differently, is equivalent to the one developed by Park and Bard that neglects mass transfer effects.[19] Figure 2 gives a schematic representation of choosing conditions under which there are no effects of mass transfer and thus independence of electrode size is changed. Here, η* is the difference between the OCP and the formal potential and can be interpreted as the relative reactivity of the heterogeneous reaction. By tracking where the kinetic term and potential term meet, one can follow the line and discover the maximum electrode radius under which the OCP is independent of electrode size. Note that Equation 14 is independent of the electrode size. One test of Equation 14 is that it breaks down to yield the Nernst Equation for fast heterogeneous electron transfer rates. For the fast rates to be true, $E_C^0 = E_A^0 = E^0$, or the standard potential. These reactions are generally symmetric, and so $\alpha = 0.5$. Also, at equilibrium, the forward and backward rates are equal. Thus, Equation 14 becomes

$$E_{OCP} = \frac{RT}{F}\ln\left[\frac{C_O^*}{C_R^*}\right] + E^0 \qquad \text{Eq. 15}$$

which is the Nernst Equation. The E^0 can be corrected for pH if the electron transfer reactions are pH-dependent by:

$$E_{pH}^0 = E^0 - 2.3\left(\frac{RT}{F}\right)(\text{-}\log_{10}[H_3O^+]) \qquad \text{Eq. 16}$$

We are interested in multicomponent systems. In the experiments conducted by Percival and Bard[20], a fast redox couple, ferrocyanide/ferricyanide was used in equimolar amounts. The OCP was monitored as a function of the concentration of ferrocyanide and ferricyanide. As the concentrations decreased, the authors observed that the OCP would change and that other reactions would begin dominating the OCP measurement. The authors hypothesized that the reactions contributing to the OCP were water oxidation and oxygen reduction in a solution that had been bubbled extensively with argon. The authors were able to account for their results by solving Equations 12 and 13 iteratively to calculate E_{OC}; however, a closed-form expression for E_{OC} is solvable and can be used to evaluate complex systems like the cell lysate and supernatant. From these considerations, any semi-quantitative treatment of the results should qualitatively and semi-quantitatively explain how the E_{OC} varies as a function of concentration of redox molecules used.

We begin by considering a solution where two reactions are contributing to the anodic current and two reactions to the cathodic current. From an analysis of a four-component system, we can eventually extrapolate to a more general expression:

Cathodic:	$O_1 + n_{C,1}e^- \rightarrow R'_1$	$E^0_{C,1}$	Eq. 17
	$O_2 + n_{C,2}e^- \rightarrow R'_2$	$E^0_{C,2}$	Eq. 18
Anodic:	$R_1 - n_{A,1}e^- \rightarrow O'_1$	$E^0_{A,1}$	Eq. 19
	$R_2 - n_{A,2}e^- \rightarrow O'_2$	$E^0_{A,2}$	Eq. 20

The OCP is now governed by four separate reactions. Thus, the condition for the equilibrium potential is:

$$|i_{A,tot}| = |i_{C,tot}| \equiv |i_{A,1}| + |i_{A,2}| = |i_{C,1}| + |i_{C,2}| \qquad \text{Eq. 21}$$

From Equations 10 and 11 above, we arrive at the following for a four-component system.

$$\frac{i_{dC,1}}{\frac{m_{O,1}}{k^0_{C,1}} e^{\alpha_{c,1} f\left(E_{OCP} - E^0_{C,1}\right)}} + \frac{i_{dC,2}}{\frac{m_{O,2}}{k^0_{C,2}} e^{\alpha_{c,2} f\left(E_{OCP} - E^0_{C,2}\right)}} = \frac{i_{dA,1}}{\frac{m_{R,1}}{k^0_{A,1}} e^{-(1-\alpha_{A,1}) f\left(E_{OCP} - E^0_{A,1}\right)}} + \frac{i_{dA,2}}{\frac{m_{R,2}}{k^0_{A,2}} e^{-(1-\alpha_{A,2}) f\left(E_{OCP} - E^0_{A,2}\right)}} \qquad \text{Eq. 22}$$

Algebraically, this equation is impossible to simplify and solve for E_{OCP}. The difficulty lies in separating the E_{OCP} values from the respective transfer coefficients (i.e., $\alpha_{C,1}$ and $\alpha_{C,2}$ & $\alpha_{A,1}$ and $\alpha_{A,2}$). One may obtain an oversimplified closed-form equation by assuming $\alpha = 0.5$.

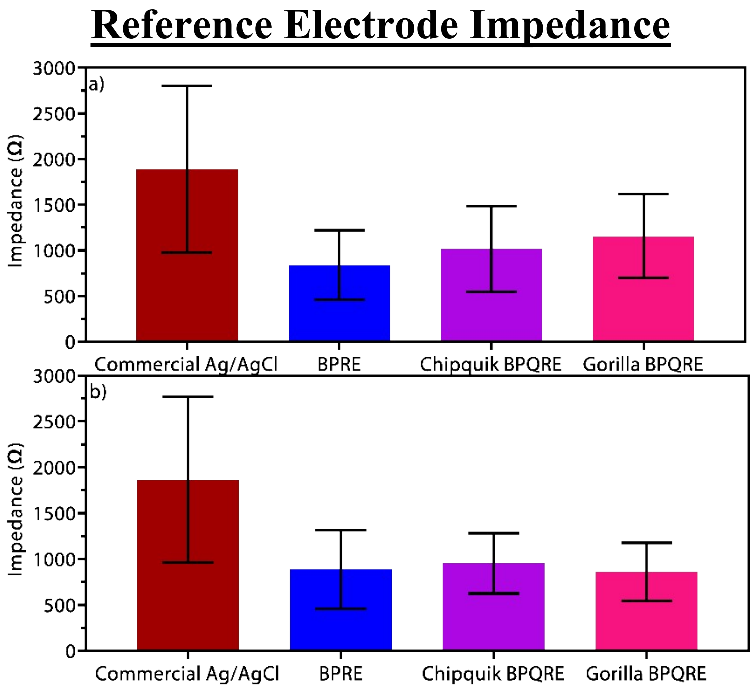

Figure 26. The reference electrode impedance measured using electrochemical impedance spectroscopy in a solution of 1M KCl, with a commercial Ag/AgCl reference electrode, a graphite rod counter electrode, and a type of reference electrode as the working electrode. **a)** in potentiostatic mode, **b)** in galvanostatic mode.

Reference impedance was measured using electrochemical impedance spectroscopy (EIS) a BioLogic VSP-300. A commercial Ag/AgCl reference electrode, a graphite rod counter electrode, and either a Au macroelectrode (*r* = 2mm) or a type of reference electrode was used as the working electrode. Measurements were taken in a solution of 1M KCl in both potentiostatic and galvanostatic modes. Using the measurement taken with the Au macroelectrode, the solution resistance of the solution was taken to be 17.5Ω in galvanostatic mode and 20.2Ω in potentiostatic mode (as determined by fitting the trace to a standard Randles cell). For measurements taken using the various types of reference electrodes as working electrodes, the impedance of the reference electrode is taken as the impedance where the phase angle is minimized with the solution resistance calculated previously removed. The measured reference electrode impedances are all statistically the same, according to an ANOVA.

Table S6. Reference Electrode Impedance

	Impedance	
Reference Tested	**Potentiostatic Mode**	**Galvanostatic Mode**
Commercial Ag/AgCl	1890 ± 920 Ω	1870 ± 900 Ω
BPRE	840 ± 380 Ω	890 ± 430 Ω
Chipquik BPQRE	1020 ± 470 Ω	950 ± 330 Ω
Gorilla BPQRE	1160 ± 460 Ω	860 ± 320 Ω

Using the BPRE with Various Electrochemical Technqiues

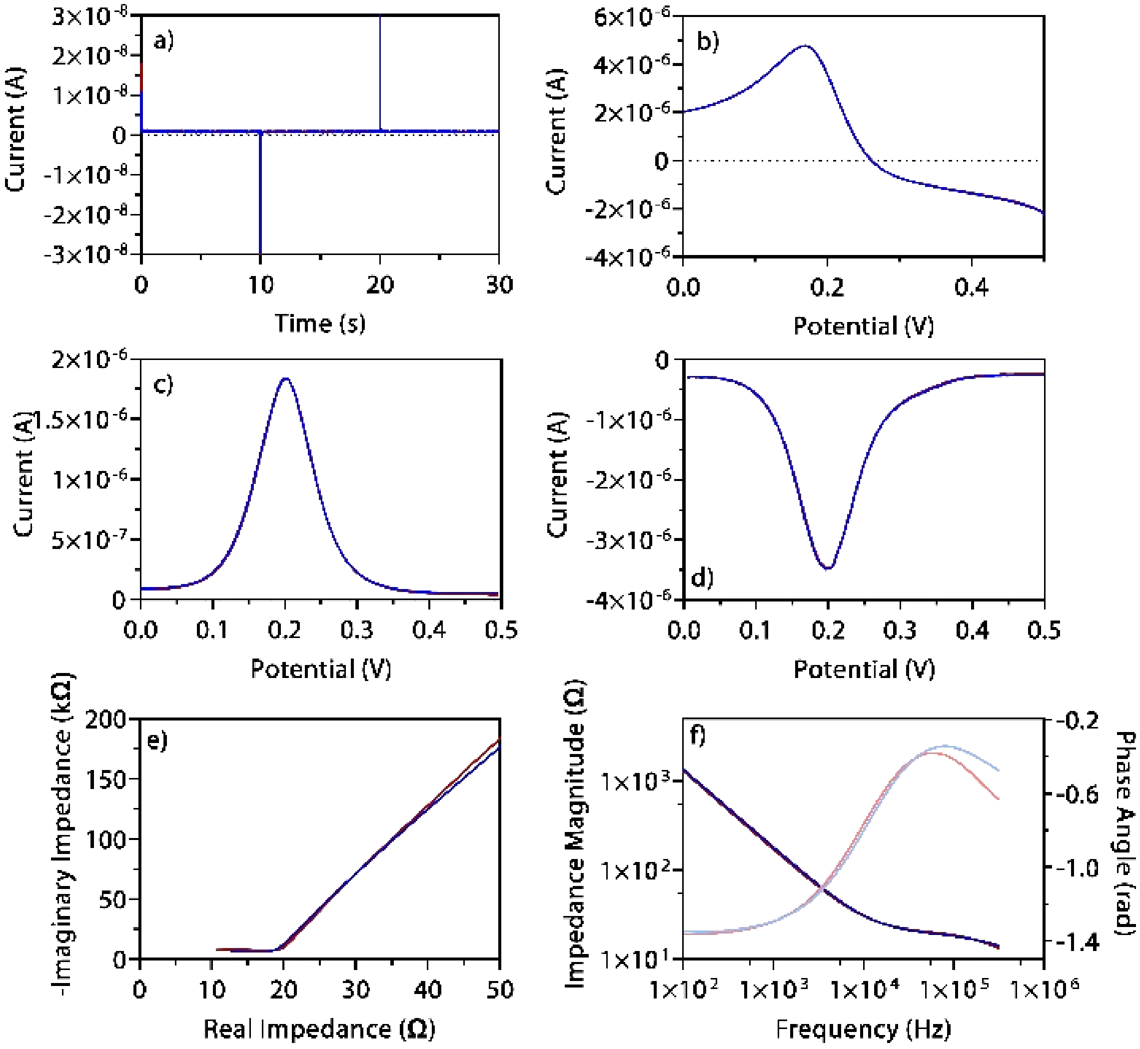

Figure S27. Example traces of solutions of 1 mM ferrocenemethanol in 250 mM KCl using a gold macroelectrode, a glassy carbon counter electrode, and either a commercial Ag/AgCl reference electrode (**red**) or a platinum BPRE (**blue**) when the measurement is **a)** differential pulse voltammetry, **b)** linear sweep voltammetry, **c)** square wave voltammetry and **d)** chronoamperometry. and **e)** electrochemical impedance spectroscopy **e)** Bode plot and **f)** Nyquist plots in a solution of 12.5 mM ferricyanide and 12.5 mM ferrocyanide in 1 M KCl using a gold macroelectrode, a glassy carbon counter electrode, and either a commercial Ag/AgCl reference electrode (**reds**) or a BPRE (**blues**).

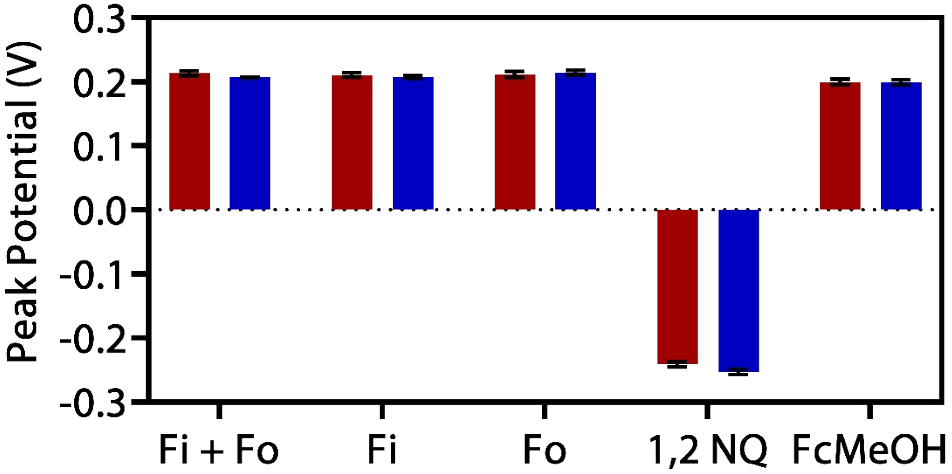

Figure S28. Differential Pulse Voltammetry results from solutions of 1 mM mediator in 250 mM KCl using a gold macroelectrode, glassy carbon counter electrode, and either a commercial Ag/AgCl reference electrode (**red**, n = 4) or a BPRE (**blue**, n = 8). Increment = 0.004 V, amplitude = 0.005 V, pulse width = 0.01 s, pulse period = 0.5 s.

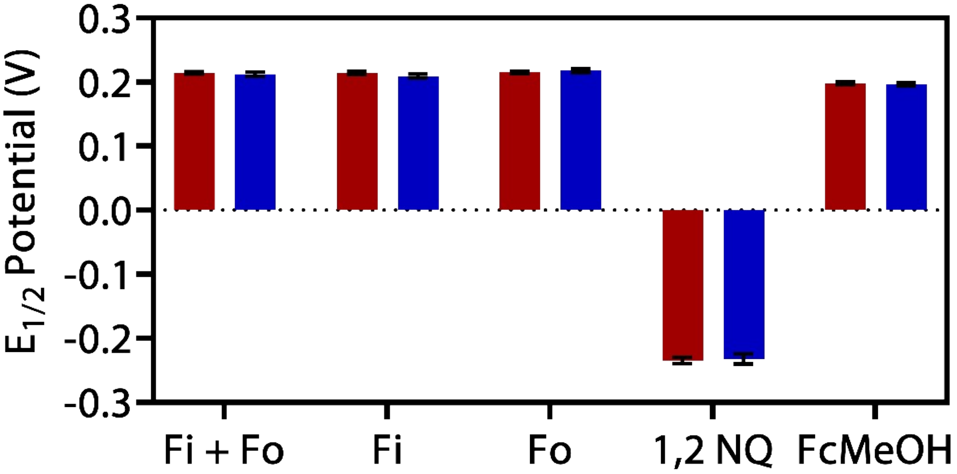

Figure S29. Linear Sweep Voltammetry results from solutions of 1 mM mediator in 250 mM KCl using a gold macroelectrode, glassy carbon counter electrode, and either a commercial Ag/AgCl reference electrode (**red**, n = 4) or a BPRE (**blue**, n = 8). Scan rate = 0.05 V/s.

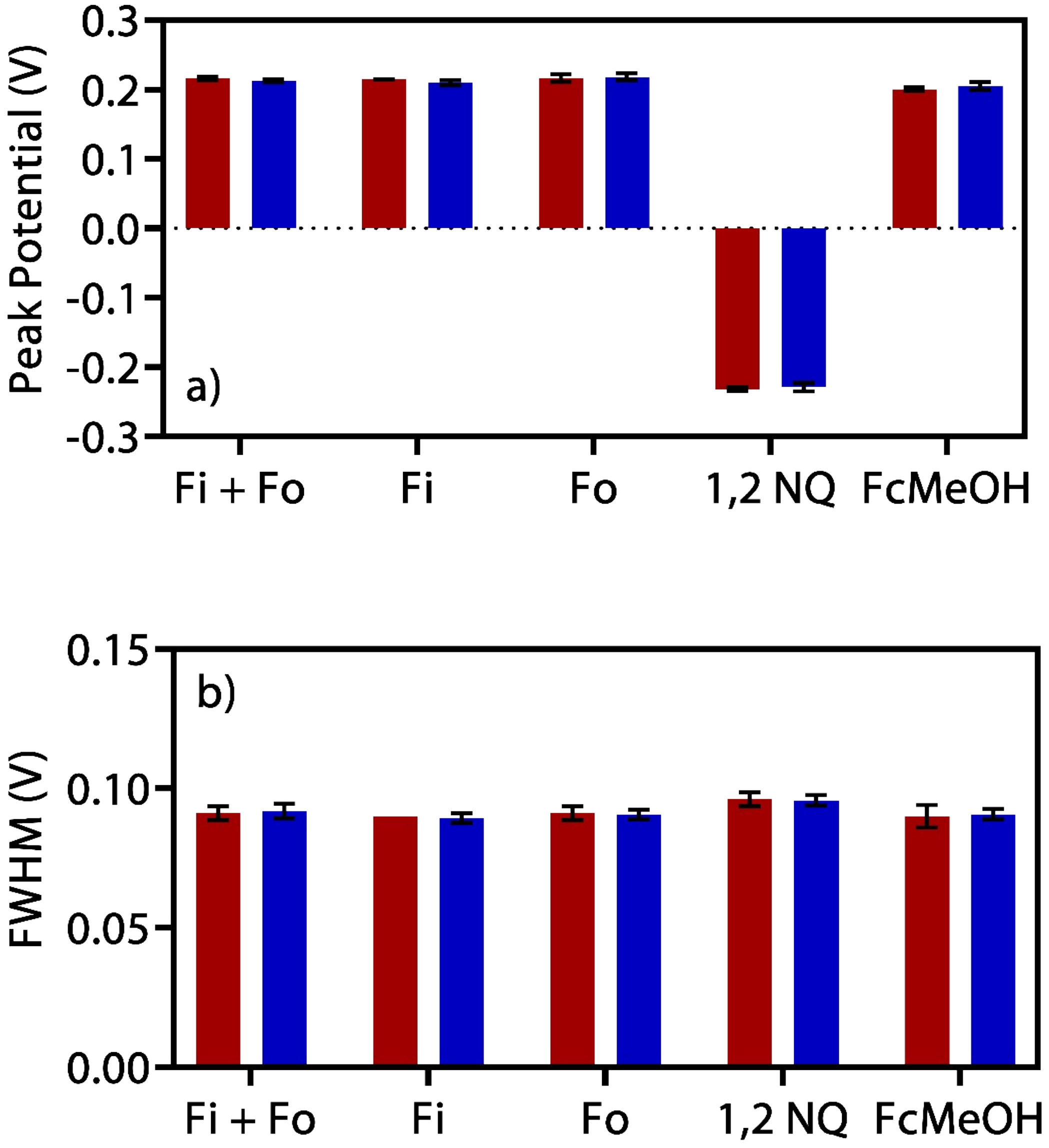

Figure S30. Square Wave Voltammetry results from solutions of 1 mM mediator in 250 mM KCl using a gold macroelectrode, glassy carbon counter electrode, and either a commercial Ag/AgCl reference electrode (**red**, n = 4) or a BPRE (**blue**, n = 8). Increment = 0.005 V, amplitude = 0.01 V, frequency = 1 Hz.

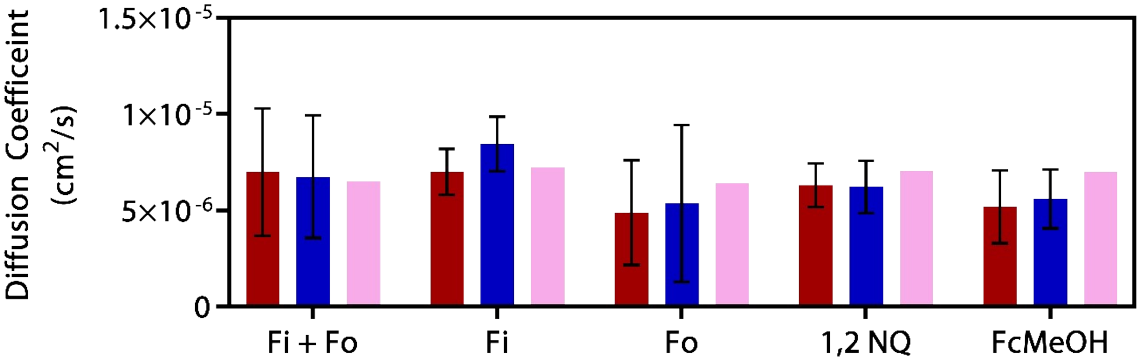

Figure S31. Chronoamperometry results from solutions of 1 mM mediator in 250 mM KCl using a gold microelectrode, glassy carbon counter electrode, and either a commercial Ag/AgCl reference electrode (**red**, n = 4) or a BPRE (**blue**, n = 8). The **pink** bars are the literature values for the diffusion coefficient. Number of steps = 3, pulse width = 10 s, sample interval = 0.001 s.

Diffusion coefficients calculated from the method described in the work of Denault et al.[21] using a gold microelectrode (r = 12.5 μm) from CHI (CH Instruments, Austin, TX). Literature sources for the diffusion coefficients are from the following sources: ferricyanide and ferrocyanide[22], ferrocenemethanol[23], and 1,2-naphthoquinone[24].

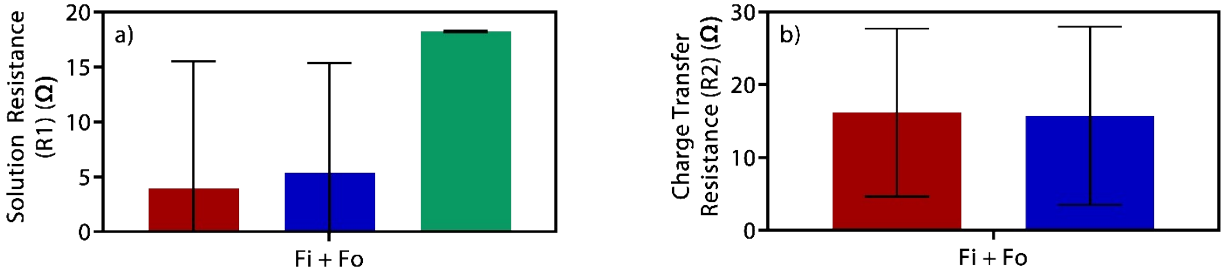

Figure S32. Electrochemical impedance spectroscopy results from solutions of 12.5 mM ferricyanide and 12.5 mM ferrocyanide in 1 M KCl using a gold macroelectrode, glassy carbon counter electrode, and either a commercial Ag/AgCl reference electrode (**red**, n = 5) or a BPRE (**blue**, n = 7). For part a, the **green** was measured using a Thermo Scientific Orion Versa Star Pro Meter (n = 5).

Measurements taken with a 530pF capacitor acting as a high frequency shunt for the reference electrode[25], with all electrodes held at the same position within the electrochemical cell between different measurements. Measurement done from 0.32 MHz to 100 Hz with an AC amplitude of 10 mV from peak to peak. Bode and Nyquist plots are fit to the circuit below (a modification of the Randles cell[26]) in order to obtain a value for **a)** solution resistance (R1) and **b)** charge transfer resistance from the surface of the electrode to the electron mediator. Here, Q1 is an imperfect capacitor representing double layer capacitance and Q2 is an imperfect capacitor representing the Warburg diffusion element[27,28].

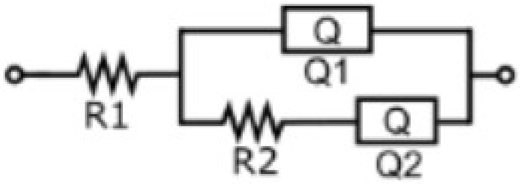

Solution resistance was measured using a Thermo Scientific Orion Versa Star Pro Meter, and using the manufacturer's conversion factor of 0.4724 cm^{-1}, resulted in a measured solution resistance of 18.25 ± 0.09 Ω (n = 5).

Data from Other Labs: CleanGrow

A few BPREs were sent to Aptisens/CleanGrow Europe (Cambridge, UK) as a possible solution for tests involving the reference being dry for periods of time.

Their CG200 Self-Calibrating-Auto Sampling 8 Ion/fertilizer Analyzer can be installed near a main feed tank in a greenhouse, and depending on how often the customer wants to measure the tank (daily, weekly, etc.) the flow cell is dry for that length of time. It would also be dry if the customer decided to put it on a shelf for a few months between uses. Depending on the environmental conditions, the currently used reference electrode has the potential to dry out. CleanGrow was interested in determining if our BPRE, which does not have a frit and therefore cannot dry out, would be a viable alternative.

Platinum reference electrode report

To test the sensor, it was installed into our CG200 Self-Calibrating-Auto Sampling 8 Ion/fertilizer Analyzer. This unit has an internal flow cell and pumps. The operating system will simultaneously calibrate and test a sample using 8 in-built solid state ion selective electrodes for calcium, potassium, magnesium, ammonium, nitrate, phosphate, chloride and sodium ions. Our ISEs are solid state using standard polymeric membranes drop cast on to a layer of CNTs deposited on a polished copper wired enclosed in a PVC housing. The calibration solution used is a multi-ion complex containing all the ions present in a hydroponic fertilizer solution in these ratios.

Table S7. Ion ratios in hydroponic fertilizer solution used as calibration solution.

	Cal low	Cal high
		ppm
Ca	15	150
K	21	210
Mg	4	40
NH4	2.035	20.35
NO3	81.94	819.4
HPO4	14.936	149.36
Cl	15	150
Na	10	100

Our usual reference electrode is a leakless miniature ag/agcl2 from Innovative Instruments Florida www.2in.com.

We expect near to full Nernstian slopes using this sensor. We compared with the 2in reference by connecting it to our CleanGrow modified handheld probe and connecting a channel to the leakless BPRE sent to us from the authors of the paper; Anal Chem. 2021 Jul 27;93(29):10065-10074. doi: 10.1021/acs.analchem.1c00675. Epub 2021 Jul 15. *We would expect close to zero potential difference between two similar reference electrodes with comparable potential, and this is what we observed.*

The sensors were not brand new, and in a multi-ion solution in a hydroponics set up it is not always possible to get the maximum slopes one would expect in a laboratory set-up with single salt solutions. In the testing we did so far it could be concluded that this BPRE would adequately replace a commercial RE in a real-world situation. *We used the calibration resulting from the slopes above with the BPRE to measure a known solution and got the expected results +/- 10%.*

References

1 E. L. Anderson, T. P. Lodge, T. Gopinath, G. Veglia and P. Bühlmann, More than a Liquid Junction: Effect of Stirring, Flow Rate, and Inward and Outward Electrolyte Diffusion on Reference Electrodes with Salt Bridges Contained in Nanoporous Glass, *Anal. Chem.,* 2019, **91**, 7698−7704.

2 A. A. Karyakin, E. E. Karyakina and L. Gorton, On the mechanism of H_2O_2 reduction at Prussian Blue modified electrodes., *Electrochem. Comm.,* 1999, **1**, 78-82.

3 M. Gautam, K. Poudel, C. S. Yong and J. O. Kim, Prussian blue nanoparticles: Synthesis, surface modification, and application in cancer treatment., *Int. J. Pharm.,* 2018, **549**, 31-49.

4 R. D. Shannon, *Acta Cryst.,* 1976, **A32**, 751-767.

5 N. L. Walker and J. E. Dick, Leakless, Bipolar Reference Electrodes: Fabrication, Performance, and Miniaturization, *Anal. Chem*., 2021, **93** (29), 10065-10074.

6 C. Lämmel, C. Heubner, T. Liebmann and M. Schneider, Critical Impact of Chloride Containing Reference Electrodes on Electrochemical Measurements, *Electroanalysis,* 2017, **29** (21), 2752-2756.

7 K. Y. Leung and C. C. L. McCrory, Effect and Prevention of Trace Ag^+ Contamination from Ag/AgCl Reference Electrodes on CO_2 Reduction Product Distributions at Polycrystalline Copper Electrodes, *ACS Appl. Energy Mater.,* 2019, **2** (11), 8283-8293.

8 M. P. S. Mousavi, S. A. Saba, E. L. Anderson, M. A. Hillmyer and P. Bühlmann, Avoiding Errors in Electrochemical Measurements: Effect of Frit Material on the Performance of Reference Electrodes with Porous Frit Junctions, *Anal. Chem.,* 2016, **88** (17), 8706-8713.

9 E. L. Anderson, B. K. Troudt and P. Bühlmann, Easy-to-Make Capillary-Based Reference Electrodes with Controlled, Pressure-Driven Electrolyte Flow, *ACS Sensors*, 2021, **6** (6), 2211-2217.

10 A. J. Bard and L .R Faulkner, Conductance, Transference Numbers, and Mobility. In *Electrochemical Methods: Fundamentals and Applications,* 2nd ed., John Wiley & Sons, Inc., 2001, 65-69.

11 A. J. Bard and L .R Faulkner, Calculation of Liquid Junction Potentials. In *Electrochemical Methods: Fundamentals and Applications,* 2nd ed., John Wiley & Sons, Inc., 2001, 69-72.

12 W. Zhan, J. Alvarez, R. M. Crooks, Electrochemical Sensing in Microfluidic Systems Using Electrogenerated Chemiluminescence as a Photonic Reporter of Redox Reactions, *J. Am. Chem. Soc.,* 2002, **124**, 13265−13270.

13 M. Hesari and Z. Ding, Review—Electrogenerated Chemiluminescence: Light Years Ahead, *J. Electrochem. Soc.,* 2016, **163**, H3116−H3131.

14 V. Eßmann, S. Voci, G. Loget, N. Sojic, W. Schuhmann and A. Kuhn, Wireless Light-Emitting Electrochemical Rotors, *J. Phys. Chem. Lett.,* 2017, **8** (19), 4930–4934.

15 A. L. Dauphin, A. Akchach, S. Voci, A. Kuhn, G. Xu, L. Bouffier and N. Sojic, Tracking Magnetic Rotating Objects by Bipolar Electrochemiluminescence, *J. Phys. Chem. Lett.,* 2019**, 10** (18), 5318-5324.

16 L. De Cola, C. W. Hsu, E. Longhi, S. Sinn, C. S. Hawes, S. Young and P. Kruger, Pyrazolo[4,3-h]quinoline Ligand-Based Iridium(III) Complexes for Electrochemiluminescence, *Chem. Asian J.,* 2017, **12** (13), 1649-1658.

17 T. D. Santa Cruz, D. L. Akins and R. L. Birke, Chemiluminescence and Energy Transfer in Systems of Electrogenerated Aromatic Anions and Benzoyl Peroxide, *J. Am. Chem. Soc.,* 1976, **98** (7), 1677-1682.

18 F. Zinna, S. Voci, L. Arrico, E. Brun, A. Homberg, L. Bouffier, T. Funaioli, J. Lacour, N. Sojic, and L. Di Bari, Circularly-Polarized Electrochemiluminescence from a Chiral Bispyrene Organic Macrocycle, *Angew. Chem. Int. Ed.,* 2019, **58**, 6952-6956.

19 J. H. Park, H. Zhou, S. J. Percival, B. Zhang, F. R. F. Fan and A. J. Bard, Open Circuit (Mixed) Potential Changes Upon Contact Between Different Inert Electrodes–Size and Kinetic Effects, *Anal. Chem*., 2013, **85**, 964-970.

20 S. J. Percival and A. J. Bard, Ultra-Sensitive Potentiometric Measurements of Dilute Redox Molecule Solutions and Determination of Sensitivity Factors at Platinum Ultramicroelectrodes, *Anal. Chem,*. 2017, **89**, 9843-9849.

21 G. Denault, M. V. Mirkin and A. J. Bard, Direct determination of diffusion coefficients by chronoamperometry at microdisk electrodes, *J. Electoanal. Chem.,* 1991, **308**, 27-38.

22 J. Moldenhauer, M. Meier and D. W. Paul, Rapid and Direct Determination of Diffusion Coefficients Using Microelectrode Arrays, *J. Electrochem. Soc.,* 2016, **163** (8), H672.

23 C. Cannes, F. Kanoufi and A. J. Bard, Cyclic voltammetry and scanning electrochemical microscopy of ferrocenemethanol at monolayer and bilayer-modified gold electrodes*, J. Electroanal. Chem.,* 2003, **547***,* 83-91.

24 M. Abdallah, A. Alharbi, M. Morad, A. M. Hameed, S. S. Al-Juaid, N. Foad and E. M. Mabrouk, Electrochemical Studies and the Electrode Reaction Mechanism of Ferrocene and Naphthoquinones in Microemulsion Medium at GC Electrode, *Int. J. Electrochem. Sci.,* 2020, **15**, 6522 – 6548.

25 F. Mansfeld, S. Lin, Y. C. Chen and H Shih, Minimization of High Frequency Phase Shifts in Impedance Measurements, *J. Electrochem. Soc.,* 1988, **135** (4), 906-907.

26 J. E. B. Randels, Kinetics of rapid electrode reactions, *Discuss. Faraday Soc.,* 1947, **1**, 11-19.

27 Basics of Electrochemical Impedance Spectroscopy; Application Note for Gamry Instruments, Incorporated: Warminster, PA, 2014,1-17.

28 A. Lasia, The Origin of the Constant Phase Element, *Phys. Chem. Lett.,* 2022, **13** (2), 580–589.